POLITECNICO DI TORINO

POLITECNICO DI TORINO

Master Degree course in Ingegneria Matematica

Master Degree Thesis

Developments in the a posteriori error analysis for the Stokes equation in the Virtual Element framework

Supervisors
Prof. Fabio Vicini
Dr. Davide Fassino

Candidate
Alessandro Di Grazia

Academic Year 2025-2026

Abstract

A posteriori error analysis for the Adaptive Virtual Element Method traditionally includes in the error estimator the stabilization term of the Virtual Element discrete space. The objective of this thesis is to prove that this stabilization term is bounded above by a stabilization-free a posteriori error estimator for the two-dimensional Stokes problem. This work is inspired by recent developments on the same topic for the classic elliptic problem. To this end, the analysis is restricted to triangular meshes with aligned edges, where only a bounded number of hanging nodes are generated during the refinement process. The a posteriori error estimator was implemented to compare the performance of the stabilization-free and the standard upper bounds. Both theoretical and numerical results confirm that, also in the Stokes framework, the stabilization term can be removed from the error estimate without loss of reliability.

Contents

Introduction

The Stokes problem describes the behavior of a steady incompressible flow with very low Reynolds number. The analytical solution of the Stokes problem is not known a priori in the general case. Moreover, complex polygonal geometries and discontinuities in the boundary condition lead to strong variations in some specific areas of the domain. In these cases, uniform meshes cause large errors in those areas; for this reason adaptive methods have become of increasing importance.

The Virtual Element Method (VEM) has been first introduced in [5] and [4] and has been developed, over the last decade, as an alternative and improved version of the Finite Element Method (FEM), to solve partial differential equations for a large variety of problems. The idea of VEM is to build a versatile scheme that works on a generic polygonal element. This is done by taking punctual values of the approximated functions only on the edges of the element, whereas the internal values of the virtual functions are unknown.

The VEM approach for the Stokes problem has been developed recently in [11], [16]; unlike the FEM, this approach has the advantage of giving an exact divergence free solution for the velocity, granting a greater numerical stability. Furthermore, the VEM approach turns out to be very practical in the handling a triangulation $\mathcal{T}$ generated in the refinement process

$$\text{SOLVE} \rightarrow \text{ESTIMATE} \rightarrow \text{MARK} \rightarrow \text{REFINE}$$

from a mesh $\mathcal{T}_0$. Indeed, when an element is refined, aligned edges are formed and a triangular element of the partition $\mathcal{T}$ is considered a polygon with more than three edges. Thus, adaptive VEM can minimize the error of the solution while keeping a lower number of cells compared to the adaptive FEM.

A fundamental idea of adaptive methods is to introduce a new quantity $\eta_{\mathcal{T}}$ called a posteriori error estimator that acts both as an upper and a lower bound for the total error. On VEM, the error estimate relies on the stabilization term $S_{\mathcal{T}}$, which is required in the discrete formulation of the problem to grant the coercivity and is a measure of the inconsistency of the VEM function with respect to a polynomial function in the error estimate. Stabilization term can be problematic as it is not consistent with the polynomial degree of the VEM amd it may be overestimated when a refined edge is much smaller than the characteristic length of an element. The novelty of this thesis is the proof that the stabilzation term $S_{\mathcal{T}}$ can be bounded from the top by the a posteriori error estimator $\eta_{\mathcal{T}}$ in the VEM formulation for the Stokes problem, allowing us to erase the stabilization

term from the error bound. This is done by adapting to the Stokes problem the work done on the classical laplacian problem in [2] and [9].

The thesis is organized as follows: chapter 1 contains the continuous and the VEM formulation of the Stokes problem problem as well as the construction of the a posteriori error estimator. The new theoretical results about the upper bound for the stabilization are presented in chapter 2. Finally, chapter 3 provides a numerical test to validate the theory. The computation of the a posteriori error has been implemented starting from the PolyDiM lybrary [7]. The pseudo-code of the new parts that have been implemented in the appendix A.

Chapter 1

Preliminaries

1.1 Variational approach for Stokes problem

We begin by stating the continuous form of Stokes problem. Its formulation, as well as theoretical results, are well known and described in detail in [8] and [13]. Let $\Omega \subseteq \mathbb{R}^2$ be a bounded and simply connected polygonal domain; we consider the problem

$$\begin{cases} \text{find } (\boldsymbol{u}, p) \text{ such that} \\ -\nu\Delta\boldsymbol{u} - \nabla p = \boldsymbol{f} \quad \text{in}\,\Omega, \\ \nabla\cdot\boldsymbol{u} \qquad\quad = 0 \quad \text{in}\,\Omega, \\ \boldsymbol{u} \qquad\quad = 0 \quad \text{on}\,\partial\Omega, \end{cases} \tag{1.1}$$

where $\boldsymbol{u} := (u_1, u_2)$ is the velocity field and p is the pressure. We assume that $\nu \in \mathbb{R}_+$. Let us define the spaces

$$\boldsymbol{V} \equiv [H_0^1(\Omega)]^2, \quad Q \equiv L_0^2(\Omega) := \left\{ q \in L^2(\Omega) | \int_\Omega q = 0 \right\},$$

with the norms

$$|\boldsymbol{v}|_{1,\Omega}^2 := \int_\Omega \|\nabla\boldsymbol{v}\|_2^2 \quad \forall \boldsymbol{v} \in \boldsymbol{V},$$

and

$$\|q\|_{0,\Omega}^2 = \int_\Omega q^2 \quad \forall q \in Q,$$

respectively. The homogeneous Dirichlet boundary condition is chosen here for the sake of simplicity. Now, we define the following bilinear forms $a : \boldsymbol{V}\times\boldsymbol{V} \to \mathbb{R}$ and $b : \boldsymbol{V}\times Q \to \mathbb{R}$ as

$$a(\boldsymbol{u}, \boldsymbol{v}) := \int_\Omega \nu\nabla\boldsymbol{u} : \nabla\boldsymbol{v} \quad \forall \boldsymbol{u}, \boldsymbol{v} \in \boldsymbol{V}, \tag{1.2}$$

$$b(\boldsymbol{v}, q) := \int_\Omega (\nabla\cdot\boldsymbol{v})q \quad \forall \boldsymbol{v} \in \boldsymbol{V}, q \in Q. \tag{1.3}$$

The operator $a(\cdot,\cdot)$ is bilinear, continuous, and coercive, i.e. there exist two constants $\|a\| > 0$ and $\alpha > 0$ such that

$$a(\boldsymbol{u}, \boldsymbol{v}) \le \|a\||\boldsymbol{u}|_{1,\Omega}|\boldsymbol{v}|_{1,\Omega} \quad \forall \boldsymbol{u}, \boldsymbol{v} \in \boldsymbol{V},$$

and

$$a(\boldsymbol{v},\boldsymbol{v}) \geq \alpha|\boldsymbol{v}|^2_{1,\Omega} \quad \forall \boldsymbol{v} \in \boldsymbol{V}.$$

The operator b is bilinear, continuous, and satisfies the inf-sup condition, i.e. there exist $\|b\| > 0$ and $\beta > 0$ such that

$$b(\boldsymbol{v},q) \leq \|b\||\boldsymbol{v}|_{1,\Omega}\|q\|_{0,\Omega} \quad \forall \boldsymbol{v} \in \boldsymbol{V},\ q \in Q,$$

and

$$\sup_{v\in\boldsymbol{V}} \frac{b(\boldsymbol{v},q)}{|\boldsymbol{v}|_{1,\Omega}} \geq \beta\|q\|_{0,\Omega} \quad \forall \boldsymbol{v} \in \boldsymbol{V},\ q \in Q.$$

Finally, we define the linear and continuous form $\mathcal{F} : \boldsymbol{V} \to \mathbb{R}$ defined as:

$$\mathcal{F}(\boldsymbol{v}) := \int_\Omega \boldsymbol{f}\cdot\boldsymbol{v}. \tag{1.4}$$

We make the assumption that $\boldsymbol{f} := (f_x, f_y) \in [L^2(\Omega)]^2$ so that $\mathcal{F}$ is well defined. The continuity of $\mathcal{F}$ implies that there exists a constant $\|\mathcal{F}\| > 0$ such that

$$\mathcal{F}(\boldsymbol{v}) \leq \|\mathcal{F}\||\boldsymbol{v}|_{1,\Omega} \quad \forall \boldsymbol{v} \in \boldsymbol{V}.$$

The weak formulation of the Stokes problem can be written as follows:

$$\begin{cases} \text{find } (\boldsymbol{u},p) \in \boldsymbol{V}\times Q \text{ such that} \\ a(\boldsymbol{u},\boldsymbol{v}) + b(\boldsymbol{v},p) = \mathcal{F}(\boldsymbol{v}) & \forall \boldsymbol{v} \in \boldsymbol{V}, \\ b(\boldsymbol{u},q) = 0 & \forall q \in Q. \end{cases} \tag{1.5}$$

We also define the bilinear form $\mathcal{B} : (\boldsymbol{V}\times Q)\times(\boldsymbol{V}\times Q)$ as

$$\mathcal{B}((\boldsymbol{u},p),(\boldsymbol{v},q)) := a(\boldsymbol{u},\boldsymbol{v}) + b(\boldsymbol{v},p) + b(\boldsymbol{u},q). \tag{1.6}$$

The problem (1.1) has a unique solution $(\boldsymbol{u},p) \in \boldsymbol{V}\times Q$ that satisfies

$$|\boldsymbol{u}|_{1,\Omega} + \|p\|_{0,\Omega} \lesssim \|F\|.$$

1.2 VEM discretization for Stokes problem

1.2.1 Mesh and triangular elements

Let $\mathcal{T}_0$ be a triangulation of the domain Ω and let $\mathcal{T}$ be a partition of the domain obtained from $\mathcal{T}_0$ following a finite number of iterations od the adaptive VEM paradigm

$$\text{SOLVE} \to \text{ESTIMATE} \to \text{MARK} \to \text{REFINE}.$$

More details about it are given in subsection 1.3.2 Any element E of the partition $\mathcal{T}$ is a triangular shaped element, possibly with aligned edges, and a geometric edge of E will be denoted by L. When one of the edges L of a triangular shaped element is refined, the edge L is split in two sub-edges. The VEM approach treats any of those sub-edges as

separate edges, thus an element E is considered a polygon with more than three edges (example show in Figure 1.1). The edges of a triangular element E are denoted by e and its length is h_e. The set of edges of E is denoted by $\mathcal{E}_E$. Each element $E \in \mathcal{T}$ has its characteristic length $h_E := |E|^{\frac{1}{2}}$, whereas we also define the characteristic length h of the partition $\mathcal{T}$ as

$$h := \max_{E \in \mathcal{T}} h_E.$$

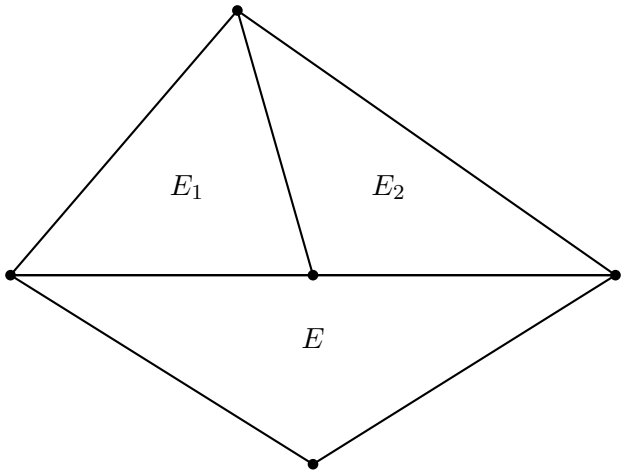

Figure 1.1. The triangle above has been refined into two triangles E_1 and E_2. The triangular shaped element E is a quadrilateral with two aligned edges.

In order to grant the validity of the results proposed in the successive discussion, the VEM approach requires the following assumption on $\mathcal{T}$:

Assumption 1. *Each triangular shaped element E must undergo the following assumption: suppose there exists a constant $\rho > 0$ such that $\forall E \in \mathcal{T}$:*

1. *E is star shaped with respect to a ball with radius greater or equal to ρh_E;*

2. *every edge $e \in \mathcal{E}_E$ has length $h_e \geq \rho h_E$.*

1.2.2 Virtual Element spaces

We proceed with the construction of the VEM method by defining the discrete space on which the discrete problem will be solved. The functions involved are all defined piecewise on the geometric elements $E \in \mathcal{T}$. First, we need to define two support spaces. Let p be a positive integer, we define

- $\mathbb{P}_p(E)$ the set of polynomials on E of degree at most p,
- $\mathcal{G}_p(E) := \nabla(\mathbb{P}_{p+1}(E)) \subseteq [\mathbb{P}_p(E)]^2$.

The local space for the velocity is the so-called *divergence-free* virtual space, and it was first introduced by [11]. Let $k \geq 2$ be the order of the VEM; for every $E \in \mathcal{T}$ we define

$$\begin{aligned}\tilde{\boldsymbol{V}}_k^E =&\{\boldsymbol{v} \in [H^1(E)]^2 : \boldsymbol{v}_{|\partial E} \in [C^0(\partial E)]^2,\, \boldsymbol{v}_{|e} \in \mathbb{P}_k(e) \forall e \in \mathcal{E}_E,\\ &\nabla \cdot \boldsymbol{v} \in \mathbb{P}_{k-1}(E), -\nu\Delta\boldsymbol{v} - \nabla s \in \mathcal{G}_{k-2}(E)^{\perp} \text{ for some } s \in L^2(E)\},\end{aligned} \tag{1.7}$$

where $\mathcal{G}_{k-2}(E)^{\perp}$ denotes the space orthogonal to $\mathcal{G}_{k-2}(E)$ with respect to the $L^2(E)$ scalar product. The dimension of the space $\tilde{\boldsymbol{V}}_k^E$ is

$$\dim(\tilde{\boldsymbol{V}}_k^E) = 2kn_E + \frac{(k-1)(k-2)}{2} + \frac{(k+1)k}{2} - 1,$$

where n_E is the number of edges and vertices of the triangular shaped element E. It is easy to verify that $[\mathbb{P}_k(E)]^2 \subseteq \tilde{\boldsymbol{V}}_k^E$. As remarked in [11], the space $\mathcal{G}_{k-2}(E)^{\perp}$ can be replaced in the definition of $\tilde{\boldsymbol{V}}_k^E$ by a space $\mathcal{G}_{k-2}(E)^{\oplus}$ such that

$$[\mathbb{P}_{k-2}(E)]^2 = \mathcal{G}_{k-2}(E) \oplus \mathcal{G}_{k-2}(E)^{\oplus}.$$

For $k \geq 1$, the following polynomial decomposition (from [3]) holds

$$[\mathbb{P}_k(E)]^2 = \mathcal{G}_k(E) \oplus \boldsymbol{x}^{\perp}\mathbb{P}_{k-1}(E), \tag{1.8}$$

where $\boldsymbol{x}^{\perp} = (x_2, -x_1)$. From now on, we take $\mathcal{G}_k(E)^{\oplus} := \boldsymbol{x}^{\perp}\mathbb{P}_{k-1}(E)$. We define the local degrees of freedom for the local spaces previously introduced. For a velocity $\boldsymbol{v} \in \tilde{\boldsymbol{V}}_k^E$, the degrees of freedom are given by:

($\mathbf{D_{v1}}$) The values of $\boldsymbol{v}$ at the vertices of the element E,

($\mathbf{D_{v2}}$) for every edge $e \subset \partial E$ the $k-1$ values of $\boldsymbol{v}$ at the $k-1$ internal points of the $k+1$ points Gauss-Lobatto quadrature rule,

($\mathbf{D_{v3}}$) the moments of order greater than 0 and up to $k-1$ of $\nabla \cdot \boldsymbol{v}$:

$$\int_E (\nabla \cdot \boldsymbol{v}) p_{k-1} \quad \forall p_{k-1} \in \mathbb{P}_{k-1}(E) \setminus \mathbb{P}_0(E),$$

($\mathbf{D_{v4}}$) the moments of $\boldsymbol{v}$:

$$\int_E \boldsymbol{v} \cdot \boldsymbol{g}_{k-2}^{\oplus} \quad \forall \boldsymbol{g}_{k-2}^{\oplus} \in \mathcal{G}_{k-2}(E)^{\oplus}.$$

We notice that the degrees of freedom ($\mathbf{D_{v4}}$) only appear for $k \geq 3$. An example of degrees of freedom for degrees $k = 2$ and $k = 3$ is shown in the Figure 1.4 . The degrees of freedom ($\mathbf{D_{v1}}$)-($\mathbf{D_{v2}}$)-($\mathbf{D_{v3}}$)-($\mathbf{D_{v4}}$) are unisolvent for the space $\tilde{\boldsymbol{V}}_k^E$.

For reasons that will be specified later, we define a new local space for velocity. This space can be obtained through the *enhancement approach*, which was first introduced in [1] and later applied to divergence free virtual spaces in [16] and [10]. For $E \in \mathcal{T}$, we first define a larger space $\boldsymbol{W}_k^E$ and for $k \geq 2$

$$\begin{aligned}\boldsymbol{W}_k^E =&\{\boldsymbol{v} \in [H^1(E)]^2 : \boldsymbol{v}|_{\partial E} \in [C^0(\partial E)]^2, \boldsymbol{v}|_e \in [\mathbb{P}_k(E)]^2 \forall e \in \mathcal{E}_E,\\ &\nabla \cdot \boldsymbol{v} \in \mathbb{P}_{k-1}(E), -\nu\Delta\boldsymbol{v} - \nabla s \in \mathcal{G}_k(E)^{\oplus} \text{ for some } s \in L^2(E)\}.\end{aligned} \tag{1.9}$$

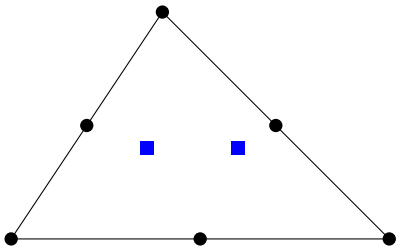

Figure 1.2. Degrees of Freedom for $k = 2$

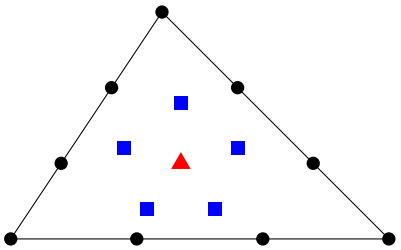

Figure 1.3. Degrees of Freedom for $k = 3$

Figure 1.4. Degrees of freedom for $k = 2$ (left) and $k = 3$ (right) for a triangular cell. The degrees of freedom on the border ($\mathbf{D_{v1}}$)-($\mathbf{D_{v2}}$) are shown in black. Internal degrees of freedom ($\mathbf{D_{v3}}$)-($\mathbf{D_{v4}}$) are shown in blue and red, respectively. For $k = 2$ ($\mathbf{D_{v4}}$) does not exist.

Then, we introduce the local enhanced divergence free virtual space:

$$\boldsymbol{V}_k^E = \left\{ \boldsymbol{v} \in \boldsymbol{W}_K^E : \int_E (\boldsymbol{v} - \Pi_k^{\nabla,E}\boldsymbol{v}) \cdot \boldsymbol{x}^\perp p = 0 \quad \forall p \in \mathbb{P}_{k-1}(E)/\mathbb{P}_{k-3}(E) \right\}, \tag{1.10}$$

where $\Pi_k^{\nabla,E} : \boldsymbol{V}_k^E \to [\mathbb{P}_k(E)]^2$ is the H^1-seminorm projection, defined by

$$\begin{cases} \int_E \nabla \Pi_k^{\nabla,E} \boldsymbol{v}_\mathcal{T} : \nabla \boldsymbol{p}_k = \int_E \nabla \boldsymbol{v}_\mathcal{T} : \nabla \boldsymbol{p}_k \quad \forall \boldsymbol{p}_k \in [\mathbb{P}_k(E)]^2, \\ \int_E \Pi_k^{\nabla,E} \boldsymbol{v}_\mathcal{T} \cdot \mathbf{1} = \int_E \boldsymbol{v}_\mathcal{T} \cdot \mathbf{1}. \end{cases} \tag{1.11}$$

The extra degrees of freedom that would be needed to identify a function in space (1.9) are set as constraints in the definition of space (1.10). It follows that

$$\dim(\boldsymbol{V}_k^E) = \dim(\tilde{\boldsymbol{V}}_k^E).$$

The degrees of freedom ($\mathbf{D_{v1}}$)-($\mathbf{D_{v2}}$)-($\mathbf{D_{v3}}$)-($\mathbf{D_{v4}}$) are unisolvent for $\boldsymbol{V}_k(E)$. The use of projections is a standard feature of VEM methods. This is justified by the fact that VEM functions cannot be known exactly except by solving a Stokes problem on the domain E. Other common projections are:

- $\Pi_k^{0,E} : \boldsymbol{V}_k^E \to [\mathbb{P}_k(E)]^2$ the L^2 projection defined by

$$\int_E \Pi_k^{0,E} \boldsymbol{v}_k \cdot \boldsymbol{p}_k = \int_E \boldsymbol{v}_k \cdot \boldsymbol{p}_k \quad \forall \boldsymbol{p}_k \in [\mathbb{P}_k(E)]^2, \tag{1.12}$$

- $\Pi_{k-1}^{0,E} \nabla : \boldsymbol{V}_k^E \to [\mathbb{P}_{k-1}(E)]^{2\times 2}$ L^2 projection of derivatives defined by

$$\int_E \left(\Pi_{k-1}^{0,E} \nabla \boldsymbol{v}_k \right) : \boldsymbol{p}_{k-1} = \int_E \nabla \boldsymbol{v}_k : \boldsymbol{p}_{k-1} \quad \forall \boldsymbol{p}_{k-1} \in [\mathbb{P}_{k-1}(E)]^{2\times 2}. \tag{1.13}$$

It can be shown that the projector $\Pi_k^{\nabla,E}$ can be computed by using the degrees of freedom ($\mathbf{D_{v1}}$)-($\mathbf{D_{v2}}$)-($\mathbf{D_{v3}}$)-($\mathbf{D_{v4}}$) for both spaces (1.7) and (1.10). This does not hold true for

operator $\Pi_k^{0,E}$. Indeed $\forall \boldsymbol{p}_k \in [\mathbb{P}_k(E)]^2$, let $q_{k+1} \in \mathbb{P}_{k+1}(E)$ and $q_{k-1} \in \mathbb{P}_{k-1}(E)$ be polynomials such that $\boldsymbol{p}_k = \nabla q_{k+1} + \boldsymbol{x}^\perp q_{k-1}$ (as follows from (1.8)). We have

$$\begin{aligned}\int_E \Pi_k^{0,E}\boldsymbol{v}\cdot\boldsymbol{p}_k &= \int_E \boldsymbol{v}\cdot\boldsymbol{p}_k \\ &= \int_E \boldsymbol{v}\cdot(\nabla q_{k+1} + \boldsymbol{x}^\perp q_{k-1}) \\ &= \int_{\partial E} \boldsymbol{v}\cdot\boldsymbol{n}(q_{k+1}) - \int_E \nabla\cdot\boldsymbol{v} q_{k+1} + \int_E \boldsymbol{v}\cdot\boldsymbol{x}^\perp q_{k-1},\end{aligned}$$

where the last integral can be computed only with the choice of the space $\boldsymbol{V}_k(E)$, since for $\tilde{\boldsymbol{V}}_k(E)$ the integral $\int_E \boldsymbol{v}\cdot\boldsymbol{x}^\perp q_{k-1}$ is known only for polynomials of degree up to $k-3$.

The local space for the pressure is taken as $Q_k^E \equiv \mathbb{P}_{k-1}(E)$, and its dimension is $\dim(Q_k)^E = \frac{(k+1)k}{2}$. For each $q \in Q_k^E$, the degrees of freedom are

($\mathbf{D_q}$) the moments of order up to $k-1$ of q:

$$\int_E q p_{k-1} \quad \forall p_{k-1} \in \mathbb{P}_{k-1}(E).$$

1.2.3 The discrete problem

We define the global VEM spaces for velocity and pressure, both defined piecewise on the elements of the mesh starting from their respective local spaces:

$$\boldsymbol{V}_\mathcal{T} = \{\boldsymbol{v} \in \boldsymbol{V} : \boldsymbol{v}|_E \in \boldsymbol{V}_k^E \,\forall E \in \mathcal{T}\}, \tag{1.14}$$

and

$$Q_\mathcal{T} = \{q \in Q : q|_E \in Q_k^E \,\forall E \in \mathcal{T}\}. \tag{1.15}$$

Now, we proceed by building the discrete stokes problem. Unlike the FEM case, it is not possible to evaluate the bilinear operator $a(\cdot,\cdot)$ on functions $\boldsymbol{v}_\mathcal{T}, \boldsymbol{w}_\mathcal{T} \in \boldsymbol{V}_\mathcal{T}$, since their exact values are not known. Thus, we evaluate the bilinear form on the projection of the functions $\boldsymbol{v}_\mathcal{T}, \boldsymbol{w}_\mathcal{T}$ onto the space $[\mathbb{P}_k(E)]^2$. For each $E \in \mathcal{T}$, we define the local bilinear form $a^E : \boldsymbol{V}_k^E \times \boldsymbol{V}_k^E \to \mathbb{R}$ as

$$a^E(\boldsymbol{u},\boldsymbol{v}) := \int_E \nu \nabla\boldsymbol{u} : \nabla\boldsymbol{v}$$

Now, we define the local discrete bilinear form $a_\mathcal{T}^E : \boldsymbol{V}_k^E \times \boldsymbol{V}_k^E \to \mathbb{R}$ as follows

$$a_\mathcal{T}^E(\boldsymbol{v}_\mathcal{T}, \boldsymbol{w}_\mathcal{T}) = a^E(\Pi_k^{\nabla,E}\boldsymbol{v}_\mathcal{T}, \Pi_k^{\nabla,E}\boldsymbol{w}_\mathcal{T}) \tag{1.16}$$

for all $\boldsymbol{v}_\mathcal{T}, \boldsymbol{w}_\mathcal{T} \in \boldsymbol{V}_k^E$. Let us introduce a local bilinear form $s^E : \boldsymbol{V}_k^E \times \boldsymbol{V}_k^E \to \mathbb{R}$. We require $s(\cdot,\cdot)$ to satisfy

$$c_S a^E(\boldsymbol{v}_\mathcal{T}, \boldsymbol{v}_\mathcal{T}) \le s^E(\boldsymbol{v}_\mathcal{T}, \boldsymbol{v}_\mathcal{T}) \le c^S a^E(\boldsymbol{v}_\mathcal{T}, \boldsymbol{v}_\mathcal{T}) \quad \forall \boldsymbol{v}_\mathcal{T} \in \boldsymbol{V}_k^E \text{ such that } \Pi_k^{\nabla,E}\boldsymbol{v}_\mathcal{T} = 0. \tag{1.17}$$

Now, we define the local stabilization form $S^E : \boldsymbol{V}_k^E \times \boldsymbol{V}_k^E \to \mathbb{R}$ defined as

$$S^E(\boldsymbol{v}_\mathcal{T}, \boldsymbol{w}_\mathcal{T}) := s^E((I - \Pi_k^{\nabla,E})\boldsymbol{v}_\mathcal{T}, (I - \Pi_k^{\nabla,E})\boldsymbol{w}_\mathcal{T}), \tag{1.18}$$

where I is the identity operator. The stabilization form is needed to ensure the coercivity of the discrete bilinear operator on functions such that $\Pi_k^{\nabla,E}\boldsymbol{v}_\mathcal{T} = 0$. There are many possible choices for the stabilization form, the most common one being the *dofi-dofi*

$$s^E(\boldsymbol{v}_\mathcal{T}, \boldsymbol{w}_\mathcal{T}) = \sum_{i=1}^{\dim(\boldsymbol{V}_k^E)} \mathrm{dof}_i(\boldsymbol{v}_\mathcal{T})\mathrm{dof}_i(\boldsymbol{w}_\mathcal{T}) \quad \forall \boldsymbol{v}_\mathcal{T}, \boldsymbol{w}_\mathcal{T} \in \boldsymbol{V}_k^E. \tag{1.19}$$

where $\mathrm{dof}_i(\cdot)$ denotes the value of the i-th local degree of freedom. By the definition of $a_\mathcal{T}(\cdot,\cdot)$ the following properties hold:

- *k-consistency*: for every $\boldsymbol{q}_k \in [\mathbb{P}_k(E)]$ and $\boldsymbol{v}_\mathcal{T} \in \boldsymbol{V}_k^E$, it holds that

$$a_\mathcal{T}^E(\boldsymbol{q}_k, \boldsymbol{v}_\mathcal{T}) = a^E(\boldsymbol{q}_k, \boldsymbol{v}_\mathcal{T});$$

- *stability*: there exists two constants $a_* > 0$ and $a^* > 0$ such that for every $\boldsymbol{v}_\mathcal{T} \in \boldsymbol{V}_k^E$,

$$a_* a^E(\boldsymbol{v}_\mathcal{T}, \boldsymbol{v}_\mathcal{T}) \leq a_\mathcal{T}^E(\boldsymbol{v}_\mathcal{T}, \boldsymbol{v}_\mathcal{T}) + \gamma S_\mathcal{T}(\boldsymbol{u}_\mathcal{T}, \boldsymbol{v}_\mathcal{T}) \leq a^* a^E(\boldsymbol{v}_\mathcal{T}, \boldsymbol{v}_\mathcal{T}),$$

where $\gamma > 0$ is a given parameter. Finally, the global discrete bilinear forms $a_\mathcal{T} : \boldsymbol{V}_\mathcal{T} \times \boldsymbol{V}_\mathcal{T} \to \mathbb{R}$ and $S_\mathcal{T} : \boldsymbol{V}_\mathcal{T} \times \boldsymbol{V}_\mathcal{T} \to \mathbb{R}$ are defined as the sum of all the local contributes

$$a_\mathcal{T}(\boldsymbol{v}_\mathcal{T}, \boldsymbol{w}_\mathcal{T}) = \sum_{E\in\mathcal{T}} a_\mathcal{T}^E(\boldsymbol{v}_\mathcal{T}, \boldsymbol{w}_\mathcal{T}) \quad \forall \boldsymbol{v}_\mathcal{T}, \boldsymbol{w}_\mathcal{T} \in \boldsymbol{V}_\mathcal{T}, \tag{1.20}$$

and

$$S_\mathcal{T}(\boldsymbol{v}_\mathcal{T}, \boldsymbol{w}_\mathcal{T}) = \sum_{E\in\mathcal{T}} S^E(\boldsymbol{v}_\mathcal{T}, \boldsymbol{w}_\mathcal{T}) \quad \forall \boldsymbol{v}_\mathcal{T}, \boldsymbol{w}_\mathcal{T} \in \boldsymbol{V}_\mathcal{T}, \tag{1.21}$$

Notice that the bilinear form $b(\cdot,\cdot)$ can be computed exactly. Indeed

$$b(\boldsymbol{v}_\mathcal{T}, q_\mathcal{T}) = \sum_{E\in\mathcal{T}} \int_E (\nabla \cdot \boldsymbol{v}_\mathcal{T}) q_\mathcal{T} \quad \forall \boldsymbol{v}_\mathcal{T} \in \boldsymbol{V}_\mathcal{T}, q_\mathcal{T} \in Q_\mathcal{T},$$

and, since $q_\mathcal{T}$ is a polynomial of degree up to $k-1$, the exact local contributions are known from the degrees of freedom ($\mathbf{D_{v3}}$). Finally, we construct a computable approximation for the right hand side of the discrete system. We define the approximated source term $\boldsymbol{f}_\mathcal{T}$ as

$$\boldsymbol{f}_\mathcal{T}|_E := \Pi_k^{0,E}\boldsymbol{f}|_E \quad \forall E \in \mathcal{T}. \tag{1.22}$$

The right hand side of the discrete problem is:

$$\mathcal{F}_\mathcal{T}(\boldsymbol{v}_\mathcal{T}) := \sum_{E\in\mathcal{T}} \int_E \boldsymbol{f}_\mathcal{T} \cdot \boldsymbol{v}_\mathcal{T} = \sum_{E\in\mathcal{T}} \int_E \boldsymbol{f} \cdot \Pi_k^{0,E}\boldsymbol{v}_\mathcal{T}, \tag{1.23}$$

where the definition (1.12) of $\Pi_k^{0,E}$ has been applied in order to obtain the last integral.

We state the discrete Stokes problem

$$\begin{cases} \text{find } (\boldsymbol{u}_\mathcal{T}, p_\mathcal{T}) \in \boldsymbol{V}_\mathcal{T} \times Q_\mathcal{T} \text{ such that} \\ a_\mathcal{T}(\boldsymbol{u}_\mathcal{T}, \boldsymbol{v}_\mathcal{T}) + \gamma S_\mathcal{T}(\boldsymbol{u}_\mathcal{T}, \boldsymbol{v}_\mathcal{T}) + b(\boldsymbol{v}_\mathcal{T}, p_\mathcal{T}) = F_\mathcal{T}(\boldsymbol{v}_\mathcal{T}) & \forall \boldsymbol{v}_\mathcal{T} \in \boldsymbol{V}_\mathcal{T}, \\ b(\boldsymbol{u}_\mathcal{T}, q_\mathcal{T}) = 0 & \forall q_\mathcal{T} \in Q_\mathcal{T}, \end{cases} \tag{1.24}$$

We also define the bilinear form $\mathcal{B}_\mathcal{T} : (\boldsymbol{V}_\mathcal{T} \times Q_\mathcal{T}) \times (\boldsymbol{V}_\mathcal{T} \times Q_\mathcal{T})$ as

$$\mathcal{B}_\mathcal{T}((\boldsymbol{u}_\mathcal{T}, p_\mathcal{T}), (\boldsymbol{v}_\mathcal{T}, q_\mathcal{T})) := a_\mathcal{T}(\boldsymbol{u}_\mathcal{T}, \boldsymbol{v}_\mathcal{T}) + b(\boldsymbol{v}_\mathcal{T}, p_\mathcal{T}) + b(\boldsymbol{u}_\mathcal{T}, q_\mathcal{T}) + \gamma S_\mathcal{T}(\boldsymbol{u}_\mathcal{T}, \boldsymbol{v}_\mathcal{T}). \tag{1.25}$$

1.2.4 Theoretical results

We summarize the main theoretical (a priori) results concerning the stability and convergence of the proposed VEM framework. These results have been found in [11] for the space $\tilde{\boldsymbol{V}}_k^E$ and have been adapted for the enhancement approach in [16] and [10]. The discrete inf-sup condition holds, meaning there exists a constant $\beta_\mathcal{T} > 0$ such that

$$\sup_{\boldsymbol{v}_\mathcal{T} \in \boldsymbol{V}_\mathcal{T}} \frac{b(\boldsymbol{v}_\mathcal{T}, q_\mathcal{T})}{|\boldsymbol{v}_\mathcal{T}|_{1,\Omega}} \leq \|q_\mathcal{T}\|_{0,E}. \tag{1.26}$$

A direct consequence of the above result is the well posedness of the discrete problem.

Theorem 1. *The problem (1.24) has unique solution $(\boldsymbol{u}_\mathcal{T}, q_\mathcal{T}) \in \boldsymbol{V}_\mathcal{T} \times Q_\mathcal{T}$, satisfying*

$$|\boldsymbol{u}_\mathcal{T}|_{1,\Omega} + \|p_\mathcal{T}\|_{0,E} \lesssim \|\mathcal{F}\|. \tag{1.27}$$

Furthermore, the velocity solution is exactly divergence free. Let us define the spaces

$$\boldsymbol{Z} := \{\boldsymbol{v} \in \boldsymbol{V}_\mathcal{T} : b(\boldsymbol{v}, q) = 0 \, \forall q \in Q\},$$

and

$$\boldsymbol{Z}_\mathcal{T} := \{\boldsymbol{v}_\mathcal{T} \in \boldsymbol{V}_\mathcal{T} : b(\boldsymbol{v}_\mathcal{T}, q_\mathcal{T}) = 0 \, \forall q_\mathcal{T} \in Q_\mathcal{T}\},$$

it holds that

$$\boldsymbol{Z}_\mathcal{T} \subseteq \boldsymbol{Z}.$$

Now, we focus on the rate of convergence of the solution. We make the assumption that both the source term $\boldsymbol{f}$ and the continuous velocity solution $\boldsymbol{u}$ are in $[H^{k+1}(\Omega)]^2$ and that $p \in H^k(\Omega)$.

Theorem 2. *Let $(\boldsymbol{u}_\mathcal{T}, p_\mathcal{T}) \in \boldsymbol{V}_\mathcal{T} \times Q_\mathcal{T}$ be the solution to the problem (1.1) and $(\boldsymbol{u}_\mathcal{T}, p_\mathcal{T}) \in \boldsymbol{V}_\mathcal{T} \times Q_\mathcal{T}$ the solution of (1.2). It holds*

$$|\boldsymbol{u} - \boldsymbol{u}_\mathcal{T}|_{1,\Omega} \lesssim (h^k |\boldsymbol{u}|_{k+1,\Omega} + h^{k+1} |\boldsymbol{f}|_{k+1,\Omega}), \tag{1.28}$$

and

$$\|p - p_\mathcal{T}\|_{0,\Omega} \leq C(h^k |\boldsymbol{u}|_{k+1,\Omega} + h^k |p|_{k,\Omega} + h^{k+1} |\boldsymbol{f}|_{k+1,\Omega}). \tag{1.29}$$

1.3 Standard a posteriori analysis

The a priori error convergence we referred in the previous section are not always reliable since the derivability of the continuous solution is not known in the general case. This leads to the need of defining a new quantity, called the a posteriori error estimator, which only depends on the discrete solution and on the problem data. In this section we propose a suitable a posteriori error estimator, introduced in [18] for the VEM framework built in the previous chapter, followed by an upper and a lower bound for the problem error based on the estimator. At the end of the section, we give more detail about the AVEM paradigm.

1.3.1 A posteriori error estimator

We define the residual quantity over an element $E \in \mathcal{T}$ for the couple $(\boldsymbol{v}, q) \in \boldsymbol{V}_\mathcal{T} \times Q_\mathcal{T}$ as

$$r_\mathcal{T}(E; \boldsymbol{v}, q) := \boldsymbol{f}_\mathcal{T} + \nu \Delta \Pi_k^{\nabla, E} \boldsymbol{v} + \nabla q. \tag{1.30}$$

We also define the jump residual over an edge e of the partition $\mathcal{T}$ shared by two triangles E_1 and E_2 as

$$j_\mathcal{T}(e; \boldsymbol{v}, q) := [[\nu \nabla \Pi_k^\nabla \boldsymbol{v} + q\mathbf{I}]]_e = \sum_{i=1}^{2} (\nu \nabla \Pi_k^{\nabla, E_i} \boldsymbol{v}|_{E_i} + q|_{E_i}\mathbf{I})\boldsymbol{n}_i, \tag{1.31}$$

where $\boldsymbol{n}_i$, $i = 1{,}2$ is the normal to the edge e pointing outward to E_i and $\mathbf{I}$ is the 2×2 identity matrix. If $e \subset \partial\Omega$, we set $j_\mathcal{T}(e; \boldsymbol{v}, q) = 0$. The local error estimator over the triangle E is defined as

$$\eta_\mathcal{T}^2(E; \boldsymbol{v}, q) := h_E^2 \|r_\mathcal{T}(E; \boldsymbol{v}, q)\|_{0,E}^2 + \frac{1}{2} \sum_{e \in \mathcal{E}_E} h_E \|j_\mathcal{T}(e; \boldsymbol{v}, q)\|_{0,E}^2, \tag{1.32}$$

and the global error estimator obtained as the sum of the local contributes

$$\eta_\mathcal{T}^2(\boldsymbol{v}, q) = \sum_{E \in \mathcal{T}} \eta_\mathcal{T}^2(E; \boldsymbol{v}, q). \tag{1.33}$$

Finally, we define the local projector error for the source term

$$\mathcal{F}^2(E) = h_E^2 \|\boldsymbol{f} - \boldsymbol{f}_\mathcal{T}\|_{0,E}^2, \tag{1.34}$$

and the global projector error for the source term

$$\mathcal{F}^2 = \sum_{E \in \mathcal{T}} \mathcal{F}^2(E). \tag{1.35}$$

Next, we present two important results from [18]. The first result is that the global estimator η serves as an upper bound for the total error produced from the discrete problem. This is useful to estimate the accuracy or the convergence of a solution when the exact solution is not known.

Theorem 3. *Let $(\boldsymbol{u}, p) \in \boldsymbol{V} \times Q$ and $(\boldsymbol{u}_\mathcal{T}, p_\mathcal{T}) \in \boldsymbol{V}_\mathcal{T} \times Q_\mathcal{T}$ be the solutions of (1.1) and (1.24), respectively. Then*

$$|\boldsymbol{u} - \boldsymbol{u}_\mathcal{T}|_{1,\Omega}^2 + \|p - p_\mathcal{T}\|_{0,\Omega}^2 \leq C_{apost}(\eta(\boldsymbol{u}_\mathcal{T}, p_\mathcal{T})^2 + S_\mathcal{T}(\boldsymbol{u}_\mathcal{T}, \boldsymbol{u}_\mathcal{T}) + \mathcal{F}^2). \tag{1.36}$$

The second result is a local lower bound for the residual error estimate.

Theorem 4. *Let* $(\boldsymbol{u}, p) \in \boldsymbol{V} \times Q$ *and* $(\boldsymbol{u}_\mathcal{T}, p_\mathcal{T}) \in \boldsymbol{V}_\mathcal{T} \times Q_\mathcal{T}$ *be the solutions of* (1.1) *and* (1.24)*, respectively. It holds*

$$\eta(\boldsymbol{u}_\mathcal{T}, p_\mathcal{T})^2 \lesssim \sum_{E' \in \mathcal{B}_E} \Big(|\boldsymbol{u} - \boldsymbol{u}_\mathcal{T}|^2_{1,E'} + \|p - p_\mathcal{T}\|^2_{0,E'} + S_\mathcal{T}(\boldsymbol{u}_\mathcal{T}, \boldsymbol{u}_\mathcal{T}) + \mathcal{F}^2 + h_{E'} \|\boldsymbol{r}_\mathcal{T}(E'; (\boldsymbol{u}_\mathcal{T}, p_\mathcal{T}))\|^2_{0,E'} \Big), \tag{1.37}$$

where $\mathcal{B}_E = \{E' \in \mathcal{T} : \partial E \cap \partial E' \neq \emptyset\}$.

1.3.2 Adaptive VEM

The a posteriori estimator defined in the previous section is fundamental for the adaptive VEM strategy. The goal of the latter is to reach a more accurate approximation of a VEM problem by using the least possible grid elements. This is done by an iterative loop, introduced by [17]. Let $\mathcal{T}_0$ be the starting tessellation of the domain. For $n \geq 0$, each n-th iteration follows the following four phases paradigm:

1. **Solve**: The problem (1.2) is solved over the current mesh $\mathcal{T}_n$. This produces the solution $(\boldsymbol{u}_\mathcal{T}^{(n)}, p_\mathcal{T}^{(n)}) \in \boldsymbol{V}_k^{(n)} \times Q_k^{(n)}$.
2. **Estimate** The local estimator $\eta(E; \boldsymbol{u}_\mathcal{T}, p_\mathcal{T})$ is computed for each element $E \in \mathcal{T}_n$.
3. **Mark**: A minimal subset $\mathcal{M}_n \subseteq \mathcal{T}_n$ is chosen following the Dörfler criterion [12]:

$$\sum_{E \in \mathcal{M}_n} \eta(E; \boldsymbol{u}_\mathcal{T}, p_\mathcal{T})^2 \geq \theta \eta(\boldsymbol{u}_\mathcal{T}, p_\mathcal{T})^2, \tag{1.38}$$

   where $\theta \in (0,1)$ is a fixed parameter.
4. **Refine**: A new tessellation $\mathcal{T}_{n+1}$ is generated from $\mathcal{T}_n$ by refining the marked elements using the newest vertex bisection.

Chapter 2

Stabilization-free error estimator

In this chapter, we present the core theoretical contribution of this thesis. In the first section, we build a specific indexing for the hanging nodes and we make an assumption for the admissibility on the partition $\mathcal{T}$. In the second section, we construct two different polynomial interpolators for the VEM functions, that are used to derive a series of intermediate inequalities. In the last section, we prove the upper bound for the stabilization term. The process is an adaptation of the work in [2] and in [9] to the Stokes problem.

2.1 Node indexing and admissibility condition

We define an indexing for the nodes on the edges as [9]. Let $\hat{E}$ be a reference triangular shaped element

$$\hat{E} := \{(x, y) \in \mathbb{R}^2 : x \geq 0, y \geq 0, x + y \leq 1\},$$

and let

$$\hat{R}_{\hat{E},k} := \left\{ \left(\frac{i}{k}, \frac{j}{k} \right) \in \mathbb{R}^2 : i \geq 0, j \geq 0, i + j \leq k \right\}.$$

Given a triangular shaped element $E \in \mathcal{T}$ and let $F_E : \hat{E} \to E$ be an affine mapping, we define

$$R_{E,k} = F_E(\hat{R}_{\hat{E},k}),$$

and the set of proper nodes $\mathcal{P}_E$ of the element E as the set of $k+1$ equispaced points on ∂E

$$\mathcal{P}_E := R_{k,E} \cap \partial E.$$

Then we define the set $\mathcal{H}_E$ of hanging nodes for the element E as

$$\mathcal{H}_E := \{\boldsymbol{x} \in \partial E : \boldsymbol{x} \in \mathcal{P}'_E \text{ for some } E \neq E' \in \mathcal{T}\} \setminus \mathcal{P}_E.$$

We also denote the set of all nodes on the element E by $\mathcal{N}_E := \mathcal{H}_E \cup \mathcal{P}_E$. Then, let $\mathcal{N}$ be the set of all the nodes in the partition. A node is said to be a *proper node* for the partition $\mathcal{T}$ if it is an element of $\mathcal{P}_E$ for each element E that contains $\boldsymbol{x}$, otherwise the node is said to be a *hanging node*. The set of proper nodes and hanging nodes for

the partition $\mathcal{T}$ are denoted by $\mathcal{P}$ and $\mathcal{H}$, respectively. It is also useful to establish an indexing of the nodes. We introduce the indexing function $\lambda : \mathcal{N} \to \mathbb{N}$ defined as

- $\lambda(\boldsymbol{x}) = 0$ if $\boldsymbol{x} \in \mathcal{P}$,
- if $\boldsymbol{x} \in \mathcal{H}$, then $\boldsymbol{x}$ is generated by partitioning another segment, having endpoints $\boldsymbol{x}'$ and $\boldsymbol{x}''$; we set
$$\lambda(\boldsymbol{x}) = 1 + \max(\lambda(\boldsymbol{x}'), \lambda(\boldsymbol{x}'')).$$

An example of indexing is proposed in Figure 2.1.

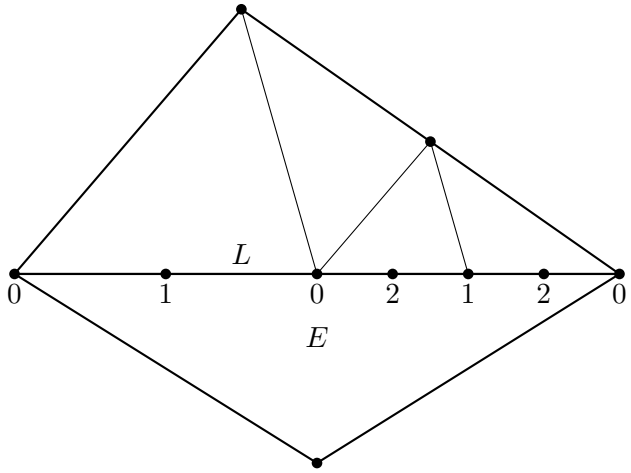

Figure 2.1. Example of indexing of the nodes of the geometric edge L of the triangle E.

On $\mathcal{T}$ we propose the following assumption from [2]:

Assumption 2. *There exists a constant $\Lambda > 0$ such that, for any partition $\mathcal{T}$ generated form refinements of $\mathcal{T}_0$, it holds*
$$\max_{\boldsymbol{x} \in \mathcal{N}} \lambda(\boldsymbol{x}) \leq \Lambda,$$

We call such a partition Λ-admissible. For a Λ admissible partition, the following properties hold

- If $L \subset \partial E$ is a geometrical edge for a triangular shaped element $E \in \mathcal{T}$, then L contains at most $2^\Lambda - 1$ hanging nodes; consequently the total number of nodes on E is bounded by $|\mathcal{N}_E| \leq 3 \cdot 2^\Lambda$.
- If $e \subset \partial E$ is an edge of $E \in \mathcal{T}$, then $|e| \simeq h_E$, where the equivalence constant depends only on $\mathcal{T}_0$ and Λ.

2.2 Local and global interpolators

We define on the triangulation $\mathcal{T}$ two additional spaces. The space of the piecewise polynomial functions
$$\mathbb{W}^k_{\mathcal{T}} := \{\boldsymbol{w} \in [L^2(\Omega)]^2 : \boldsymbol{w}|_E \in [\mathbb{P}_k(E)]^2 \, \forall E \in \mathcal{T}\}, \tag{2.1}$$

and the space of piecewise polynomial VEM functions

$$\boldsymbol{V}_{\mathcal{T}}^0 := \boldsymbol{V}_{\mathcal{T}} \cap \mathbb{W}_{\mathcal{T}}^k. \tag{2.2}$$

Moreover, we introduce the base of scaled monomial on the triangular shaped element E:

$$\mathcal{M}_k(E) = \left\{ m \in \mathbb{P}_k(E) : m(x,y) = \frac{(x-x_E)^{\alpha_x}(y-y_E)^{\alpha_y}}{h_E^{\alpha_x+\alpha_y}} \quad \forall 0 \le \alpha_x + \alpha_y \le k \right\},$$

where (x_E, y_E) denotes the centroid of the triangular shaped element E, and $\boldsymbol{\alpha} := (\alpha_x, \alpha_y)$ is a multi-index of non-negative integers. We also define the interpolation operator $\mathcal{I}_E : \boldsymbol{V}_k^E \to [\mathbb{P}_k(E)]^2$ defined by

- $\boldsymbol{v}(\boldsymbol{x}) = (\mathcal{I}_E \boldsymbol{v})(\boldsymbol{x}) \quad \forall \boldsymbol{x} \in \mathcal{P}_E$,
- $\boldsymbol{\mu}_p^{\mathrm{div}}(\boldsymbol{v}, E) = \boldsymbol{\mu}_p^{\mathrm{div}}(\mathcal{I}_E \boldsymbol{v}, E) \quad$ for $1 \le p \le k-2$,
- $\boldsymbol{\mu}_p^{\perp}(\boldsymbol{v}, E) = \boldsymbol{\mu}_p^{\perp}(\mathcal{I}_E \boldsymbol{v}, E) \quad$ for $0 \le p \le k-4$,

where $\boldsymbol{\mu}_p^{\mathrm{div}}(\boldsymbol{v}, E) : \left(\frac{1}{|E|}\int_E (\nabla \cdot \boldsymbol{v}) m\right)_{m \in \mathcal{M}_p \setminus \mathcal{M}_{p-1}}$ and $\boldsymbol{\mu}_p^{\perp}(\boldsymbol{v}, E) : \left(\frac{1}{|E|}\int_E (\boldsymbol{x}^{\perp} \cdot \boldsymbol{v}) m\right)_{m \in \mathcal{M}_p \setminus \mathcal{M}_{p-1}}$.

The set of $2N_k$ conditions given defines a unique couple of polynomials. Finally we define the interpolation operator $\mathcal{I}_{\mathcal{T}} : \boldsymbol{V}_{\mathcal{T}} \to \mathbb{W}_{\mathcal{T}}^k$ which restrict to $\mathcal{I}_E$ on each $E \in \mathcal{T}$.

Lemma 1. *Let $(\boldsymbol{u}, p)$ be the solution of (1.1) and $(\boldsymbol{u}_{\mathcal{T}}, p_{\mathcal{T}})$ be the solution to (1.24). For each $\boldsymbol{v}_{\mathcal{T}} \in \boldsymbol{V}_{\mathcal{T}}^0$, it holds*

$$\mathcal{B}((\boldsymbol{u} - \boldsymbol{u}_{\mathcal{T}}, p - p_{\mathcal{T}}), (\boldsymbol{v}_{\mathcal{T}}, q_{\mathcal{T}})) = 0. \tag{2.3}$$

Proof. We begin by adding and subtracting the first equation of (1.24),

$$\begin{aligned}\mathcal{B}((\boldsymbol{u} - \boldsymbol{u}_{\mathcal{T}}, p - p_{\mathcal{T}}), (\boldsymbol{v}_{\mathcal{T}}, q_{\mathcal{T}})) &= \mathcal{B}((\boldsymbol{u}, p), (\boldsymbol{v}_{\mathcal{T}}, q_{\mathcal{T}})) - \mathcal{B}((\boldsymbol{u}_{\mathcal{T}}, p_{\mathcal{T}}), (\boldsymbol{v}_{\mathcal{T}}, q_{\mathcal{T}})) \\ &= \mathcal{F}(\boldsymbol{v}_{\mathcal{T}}) - \mathcal{F}_{\mathcal{T}}(\boldsymbol{v}_{\mathcal{T}}) + \mathcal{B}_{\mathcal{T}}((\boldsymbol{u}_{\mathcal{T}}, p_{\mathcal{T}}), (\boldsymbol{v}_{\mathcal{T}}, q_{\mathcal{T}})) - \mathcal{B}((\boldsymbol{u}_{\mathcal{T}}, p_{\mathcal{T}}), (\boldsymbol{v}_{\mathcal{T}}, q_{\mathcal{T}})).\end{aligned}$$

By definition of $\Pi_k^{0,E}$ and since $\boldsymbol{v}_{\mathcal{T}}$ is a polynomial of degree k when restricted on a triangle E

$$\mathcal{F}(\boldsymbol{v}_{\mathcal{T}}) - \mathcal{F}_{\mathcal{T}}(\boldsymbol{v}_{\mathcal{T}}) = \sum_{E \in \mathcal{T}} \int_E \left(\boldsymbol{f} - \Pi_k^{0,E} \boldsymbol{f}\right) \cdot \boldsymbol{v}_{\mathcal{T}} = 0.$$

We show that the remaining terms in the previous equation also cancel. It holds

$$\begin{aligned}&\mathcal{B}_{\mathcal{T}}((\boldsymbol{u}_{\mathcal{T}}, p_{\mathcal{T}}), (\boldsymbol{v}_{\mathcal{T}}, q_{\mathcal{T}})) - \mathcal{B}((\boldsymbol{u}_{\mathcal{T}}, p_{\mathcal{T}}), (\boldsymbol{v}_{\mathcal{T}}, q_{\mathcal{T}})) = \\ &a_{\mathcal{T}}(\boldsymbol{u}_{\mathcal{T}}, \boldsymbol{v}_{\mathcal{T}}) + \gamma S_{\mathcal{T}}(\boldsymbol{u}_{\mathcal{T}}, \boldsymbol{v}_{\mathcal{T}}) + b(\boldsymbol{v}_{\mathcal{T}}, p_{\mathcal{T}}) + b(\boldsymbol{u}_{\mathcal{T}}, q_{\mathcal{T}}) - a(\boldsymbol{u}_{\mathcal{T}}, \boldsymbol{v}_{\mathcal{T}}) - b(\boldsymbol{v}_{\mathcal{T}}, p_{\mathcal{T}}) - b(\boldsymbol{u}_{\mathcal{T}}, q_{\mathcal{T}}) = \\ &\sum_{E \in \mathcal{T}} \left(a_{\mathcal{T}}^E(\boldsymbol{u}_{\mathcal{T}}, \boldsymbol{v}_{\mathcal{T}}) - a^E(\boldsymbol{u}_{\mathcal{T}}, \boldsymbol{v}_{\mathcal{T}}) + \gamma S_{\mathcal{T}}^E(\boldsymbol{u}_{\mathcal{T}}, \boldsymbol{v}_{\mathcal{T}})\right) = 0\end{aligned}$$

Indeed $S_{\mathcal{T}}^E(\boldsymbol{u}_{\mathcal{T}}, \boldsymbol{v}_{\mathcal{T}}) = 0$, since $\boldsymbol{v}_{\mathcal{T}}$ is a polynomial on E and $a_{\mathcal{T}}^E(\boldsymbol{u}_{\mathcal{T}}, \boldsymbol{v}_{\mathcal{T}}) = a^E(\boldsymbol{u}_{\mathcal{T}}, \boldsymbol{v}_{\mathcal{T}})$ because of the *k-consistency* property. □

Another important property that will be involved in the further discussion is the scaled Poincaré inequality.

Proposition 1. *There exists a constant $C_p > 0$, independent on $\mathcal{T}$, such that*

$$\sum_{E\in\mathcal{T}} h_E^{-2}\|\boldsymbol{v}\|_{0,E} \leq C_p|\boldsymbol{v}|_{1,\Omega} \quad \textit{for each } \boldsymbol{v}\in\boldsymbol{V}_{\mathcal{T}} \textit{ such that } \boldsymbol{v}(\boldsymbol{x}) = 0\,\forall \boldsymbol{x}\in\mathcal{P}. \tag{2.4}$$

The proof is the same as [9], since it holds for geometrical reasons. For clearness, we report it here.

Proof. It is sufficient to show that each triangle contains at least a proper node, then the result follows from the classical Poincaré inequality. We recall that we are considering the spaces of degree $k \geq 2$, meaning that each edge has at least one internal node.

Let $E \in \mathcal{T}$ be an element of the triangulation. If E is an element of the original partition $\mathcal{T}_0$, then is vertices are proper nodes. If E has been generated by splitting another triangle $\tilde{E}$ into two triangles E and E', we focus on their common edge L. If the triangle E' has not been refined, the the internal nodes on L are proper nodes. If E' has been refined and k is even, then the midpoint of L is a proper node.

If k is odd, denote with $M \geq 1$ the number of refinement on L and take the node $\boldsymbol{x}$ that lays at a distance $|L|/k$ from on of the vertices on L. Then $\boldsymbol{x}$ belongs to one of the intervals of width $|L|/2^s$ for some $1 \leq s \leq M$. That means that exists an integer $m > 0$ such that

$$\frac{|L|}{2^s}m \leq \frac{|L|}{k} \leq \frac{|L|}{2^s}(m+1)$$

or equivalently,

$$km \leq 2^s \leq k(m+1).$$

The described interval is an edge for a smaller element of the partition $\mathcal{T}$, meaning that it contains two nodes on positions

$$\frac{|L|}{2^s}\left(m + \frac{n}{k}\right) \quad n = 0, ..., k. \tag{2.5}$$

By taking $n = 2^s - mk$ we obtain the node $\boldsymbol{x}$, meaning that it is a node for both the triangles that contain it. That means that $\boldsymbol{x}$ is a proper node. □

We consider the operator $\mathcal{I}_E$ restricted on a geometric edge L of a triangular shaped element $E \in \mathcal{T}$. Let $\boldsymbol{v} \in \boldsymbol{V}_k^E$, we recall that $\boldsymbol{v}$ restricted on L is a couple of piecewise polynomials of degree k. The exact form of $\boldsymbol{v}$ on L can be determined using all the nodes on the edge L, including the nodes generated by further refinements of the edge. We also recall the the number of nodes on edge L is limited by a constant depending on Λ. We denote by J_L the maximum layer of refinement on the edge L. We write the interpolation error on the edge $(\boldsymbol{v} - \mathcal{I}_E\boldsymbol{v})|_L$ telescopically, as follows

$$(\boldsymbol{v} - \mathcal{I}_E\boldsymbol{v})|_L = \sum_{j=1}^{J_L}(\mathcal{I}_j - \mathcal{I}_{j-1})\boldsymbol{v}. \tag{2.6}$$

The operators $\mathcal{I}_j$, $j = 0, ..., J_L$ interpolate the function $\boldsymbol{v}$ on the j-th layer of partition, i.e. on the sub interval of length $\frac{|L|}{2^j}$. Specifically, $\mathcal{I}_0 \equiv \mathcal{I}_E|_L$ and $\mathcal{I}_{J_L}$ is the identity operator on L.

Now, let S be a sub-edge of length $\frac{|L|}{2^{j-1}}$ that is split on two smaller sub-edges S^+, S^- of length $\frac{|L|}{2^j}$. On S we consider

$$\mathcal{I} := \mathcal{I}_{j-1}|_S : [C^0(S)]^2 \to [\mathbb{P}_k(S)]^2,$$

and

$$\check{\mathcal{I}} := \mathcal{I}_j|_S : [C^0(S)]^2 \to [\mathbb{P}_k(S^-, S^+)]^2,$$

where

$$\mathbb{P}_k(S^-, S^+) = \left\{ v \in C^0(S) : v|_{S^-} \in \mathbb{P}_k(S^-), v|_{S^+} \in \mathbb{P}_k(S^+) \right\}.$$

Our goal is to investigate on the behavior if $(\check{\mathcal{I}} - \mathcal{I})\boldsymbol{v}$. The interpolator $\mathcal{I}$ needs $2(k+1)$ conditions to construct the polynomial couple on S. These conditions are given by the values of the two components of $\boldsymbol{v}$ in $k+1$ equispaced points $\boldsymbol{\xi}_n$, $n = 1, ..., k+1$ on the sub-edge S. The interpolator $\check{\mathcal{I}}$ needs $2(k+1)$ conditions on each of the sub-edges S^-, S^+, given by the values of the two components of $\boldsymbol{v}$ in $2k+1$ equispaced point on the sub-edge S. An example is shown in the Figure 2.2. Among those points there are $\boldsymbol{\xi}_n$, $n = 0, ..., k+1$ along with k new points $\boldsymbol{\zeta}_i$, $i = 1, ..., k$.

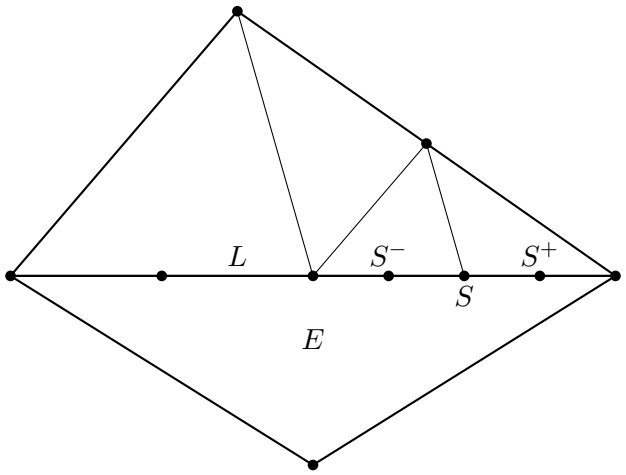

Figure 2.2. The figure shows a triangle E with a refined geometrical edge L. The sub-edge S has been generated at the first level of refinement, and the sub-edges S^- and S^+ have been generated at the secon level of refinement.

Notice that $((\check{\mathcal{I}} - \mathcal{I})\boldsymbol{v})(\boldsymbol{\xi}_n) = 0$ for each $n = 1, ..., k+1$, thus the difference $(\check{\mathcal{I}} - \mathcal{I})\boldsymbol{v}$

can be written as a linear combination of the $2k$ basis functions

$$\boldsymbol{\psi}_i^{(x)}(\boldsymbol{x}) = \begin{cases} \begin{pmatrix} 1 \\ 0 \end{pmatrix} & \text{if } \boldsymbol{x} = \boldsymbol{\zeta}_i, \\ \begin{pmatrix} 0 \\ 0 \end{pmatrix} & \text{if } \boldsymbol{x} = \boldsymbol{\zeta}_j,\ j \neq i, \\ \begin{pmatrix} 0 \\ 0 \end{pmatrix} & \text{if } \boldsymbol{x} = \boldsymbol{\xi}_n,\ n = 1, ..., k+1, \end{cases} \qquad 1 \leq i \leq k,$$

and

$$\boldsymbol{\psi}_i^{(y)}(\boldsymbol{x}) = \begin{cases} \begin{pmatrix} 0 \\ 1 \end{pmatrix} & \text{if } \boldsymbol{x} = \boldsymbol{\zeta}_i, \\ \begin{pmatrix} 0 \\ 0 \end{pmatrix} & \text{if } \boldsymbol{x} = \boldsymbol{\zeta}_j,\ j \neq i, \\ \begin{pmatrix} 0 \\ 0 \end{pmatrix} & \text{if } \boldsymbol{x} = \boldsymbol{\xi}_n,\ n = 1, ..., k+1, \end{cases} \qquad 1 \leq i \leq k.$$

Where the functions $\boldsymbol{\psi}_i^{(x)}(\boldsymbol{x})$ and $\boldsymbol{\psi}_i^{(y)}(\boldsymbol{x})$ only differ from each other by the non-zero component. Here the function $(\check{\mathcal{I}} - \mathcal{I})\boldsymbol{v}$ in each of the $\boldsymbol{\zeta}_i$, $i = 1, ..., k$ is described by two values $d_x(\boldsymbol{v}, \boldsymbol{\zeta}_i)\boldsymbol{\psi}_i^{(x)}$ and $d_x(\boldsymbol{v}, \boldsymbol{\zeta}_i)\boldsymbol{\psi}_i^{(x)}$ called *details*. On the other hand, in [2] and [9], the same function is described by a single detail in each point. All the results in the following of this section are adaptation of the ones for the classical laplacian problem based on this distinction.

We write

$$(\check{\mathcal{I}} - \mathcal{I})\boldsymbol{v} = \sum_{i=1}^{k} d_x(\boldsymbol{v}, \boldsymbol{\zeta}_i)\boldsymbol{\psi}_i^{(x)} + d_y(\boldsymbol{v}, \boldsymbol{\zeta}_i)\boldsymbol{\psi}_i^{(y)},$$

where

$$d_x(\boldsymbol{v}, \boldsymbol{\zeta}_i) := (\check{\mathcal{I}}\boldsymbol{v} - \mathcal{I}\boldsymbol{v})_x(\boldsymbol{\zeta}_i) = (v_x - (\mathcal{I}\boldsymbol{v})_x)(\boldsymbol{\zeta}_i),$$

and

$$d_y(\boldsymbol{v}, \boldsymbol{\zeta}_i) := (\check{\mathcal{I}}\boldsymbol{v} - \mathcal{I}\boldsymbol{v})_y(\boldsymbol{\zeta}_i) = (v_y - (\mathcal{I}\boldsymbol{v})_y)(\boldsymbol{\zeta}_i).$$

The values of $\mathcal{I}\boldsymbol{v}$ at the $\boldsymbol{\zeta}_i$ can be obtained from the values of $\mathcal{I}\boldsymbol{v}$ at the nodes $\boldsymbol{\xi}_i$.

$$(\mathcal{I}\boldsymbol{v})(\boldsymbol{\zeta}_i) = \sum_{n=1}^{k+1} \alpha_{i,n}\mathcal{I}\boldsymbol{v}(\boldsymbol{\xi}_n) = \sum_{n=1}^{k+1} \alpha_{i,n}\boldsymbol{v}(\boldsymbol{\xi}_n). \tag{2.7}$$

The coefficients only depend on the mutual positions of the nodes, thus, they are independent on the level of partition j. Furthermore, the coefficients are the same for the two components of the velocity. This allows us to express the coefficients $d_x(\boldsymbol{v}, \boldsymbol{\zeta}_i)$ and $d_x(\boldsymbol{v}, \boldsymbol{\zeta}_i)$ in terms of the values of $\boldsymbol{v}$.

On the edge L, if a hanging node $\boldsymbol{\zeta}$ is generated at the j-th level of refinement, the previous construction can be applied to obtain two basis functions $\boldsymbol{\psi}_{\boldsymbol{\zeta}}^{(x)}$ and $\boldsymbol{\psi}_{\boldsymbol{\zeta}}^{(y)}$ having

support only on their relative interval of length $\frac{|L|}{2^{j-1}}$. Their respective coefficients can be obtained as well

$$d_x(\boldsymbol{v}, \boldsymbol{\zeta}) = (v_x - (\mathcal{I}_{j-1}\boldsymbol{v})_x)(\boldsymbol{\zeta}),$$

and

$$d_y(\boldsymbol{v}, \boldsymbol{\zeta}) = (v_y - (\mathcal{I}_{j-1}\boldsymbol{v})_y)(\boldsymbol{\zeta}).$$

Summing on all the levels of partition, we get the following expression for the interpolation error on the edge:

$$(\boldsymbol{v} - \mathcal{I}_E\boldsymbol{v})|_L = \sum_{\boldsymbol{\zeta}\in\mathcal{H}_L} d_x(\boldsymbol{v}, \boldsymbol{\zeta})\boldsymbol{\psi}_{\boldsymbol{\zeta}}^{(x)} + d_y(\boldsymbol{v}, \boldsymbol{\zeta})\boldsymbol{\psi}_{\boldsymbol{\zeta}}^{(y)}, \tag{2.8}$$

where $\mathcal{H}_L = \mathcal{H}_E \cap L$.

Next, we define a subspace of the space $\boldsymbol{V}_k^E$

$$\begin{aligned}\boldsymbol{X}_E := \{\boldsymbol{w} \in \boldsymbol{V}_k^E : \boldsymbol{w}(\boldsymbol{x}) = 0 \,\forall \boldsymbol{x} \in \mathcal{P}_E,\, \boldsymbol{\mu}_p^{\mathrm{div}}(\boldsymbol{w}, E) = 0,\, 1 \le p \le k-2 \\ \text{and } \boldsymbol{\mu}_p^{\perp}(\boldsymbol{w}, E) = 0,\, 0 \le p \le k-4\}.\end{aligned}$$

Consider on the space $\boldsymbol{X}_E$ the norm $|\boldsymbol{w}|_{1,E}$ and the norm

$$\|\boldsymbol{w}\|_{\boldsymbol{X}_E} = \left[\sum_{\boldsymbol{\zeta}\in\mathcal{H}_E} \left(d_x^2(\boldsymbol{w}, \boldsymbol{\zeta}) + d_x^2(\boldsymbol{w}, \boldsymbol{\zeta})\right) + |\boldsymbol{\mu}_{k-1}^{\mathrm{div}}(\boldsymbol{w}, E)|^2 + |\boldsymbol{\mu}_{k-3}^{\perp}(\boldsymbol{w}, E)|^2\right]^{\frac{1}{2}}.$$

We observe that both the dimension and the norm $\|\boldsymbol{w}\|_{\boldsymbol{X}_E}$ scales with the number of hanging nodes, which are bounded by a constant depending on Λ. This implies that the two norms are equivalent and the constant of equivalence depends only on Λ. It follows that

$$\sum_{\boldsymbol{\zeta}\in\mathcal{H}_E} \left(d_x^2(\boldsymbol{w}, \boldsymbol{\zeta}) + d_y^2(\boldsymbol{w}, \boldsymbol{\zeta})\right) \le \|\boldsymbol{w}\|_{\boldsymbol{X}_E} \simeq |\boldsymbol{w}|_{1,\Omega}, \quad \forall \boldsymbol{w} \in \boldsymbol{X}_E.$$

Since $\boldsymbol{v} - \mathcal{I}_E\boldsymbol{v} \in \boldsymbol{X}_E$, $d_x^2(\boldsymbol{v} - \mathcal{I}_E\boldsymbol{v}, \boldsymbol{\zeta}) = d_x^2(\boldsymbol{v}, \boldsymbol{\zeta})$ and $d_y^2(\boldsymbol{v} - \mathcal{I}_E\boldsymbol{v}, \boldsymbol{\zeta}) = d_y^2(\boldsymbol{v}, \boldsymbol{\zeta})$, for every $\boldsymbol{\zeta} \in \mathcal{H}_E$, we obtain

$$\sum_{\boldsymbol{\zeta}\in\mathcal{H}_E} \left(d_x^2(\boldsymbol{v}, \boldsymbol{\zeta}) + d_y^2(\boldsymbol{v}, \boldsymbol{\zeta})\right) \le |\boldsymbol{v} - \mathcal{I}_E\boldsymbol{v}|_{1,E}.$$

Finally, we sum on all the triangles to obtain the following result.

Lemma 2. *There exists a constant $C_D > 0$ depending on Λ but independent on $\mathcal{T}$ such that, for all $\boldsymbol{v} - \boldsymbol{V}_{\mathcal{T}}$*

$$\sum_{\boldsymbol{\zeta}\in\mathcal{H}} \left(d_x^2(\boldsymbol{v}, \boldsymbol{\zeta}) + d_y^2(\boldsymbol{v}, \boldsymbol{\zeta})\right) \le C_D|\boldsymbol{v} - \mathcal{I}_E\boldsymbol{v}|_{1,\mathcal{T}}. \tag{2.9}$$

Now, we introduce a new interpolation operator $\mathcal{I}_{\mathcal{T}}^0 : \boldsymbol{V}_{\mathcal{T}} \to \boldsymbol{V}_{\mathcal{T}}^0$ defined by the following conditions:

- $\boldsymbol{v}(\boldsymbol{x}) = (\mathcal{I}_{\mathcal{T}}^0\boldsymbol{v})(\boldsymbol{x}) \quad \forall \boldsymbol{x} \in \mathcal{P}$,

- $\boldsymbol{\mu}_p^{\mathrm{div}}(\boldsymbol{v}, E) = \boldsymbol{\mu}_p^{\mathrm{div}}(\mathcal{I}_{\mathcal{T}}^0 \boldsymbol{v}, E) \quad$ for $1 \le p \le k-2$ and $\forall E \in \mathcal{T}$,
- $\boldsymbol{\mu}_p^{\perp}(\boldsymbol{v}, E) = \boldsymbol{\mu}_p^{\perp}(\mathcal{I}_{\mathcal{T}}^0 \boldsymbol{v}, E) \quad$ for $0 \le p \le k-4$ and $\forall E \in \mathcal{T}$.

The operator is well defined since if an element $E \in \mathcal{T}$ has an hanging nodes, the value of $\mathcal{I}_{\mathcal{T}}^0 \boldsymbol{v}$ on the hanging node is obtained recursively following the same construction presented at the beginning of this section.

The following lemma gives a representation of the difference between the two operators:

Lemma 3. *It holds*

$$|\mathcal{I}_{\mathcal{T}} \boldsymbol{v} - \mathcal{I}_{\mathcal{T}}^0 \boldsymbol{v}|_{1,\mathcal{T}}^2 \simeq \sum_{\boldsymbol{\zeta} \in \mathcal{H}} \left(\delta_x^2(\boldsymbol{v}, \boldsymbol{\zeta}) + \delta_y^2(\boldsymbol{v}, \boldsymbol{\zeta}) \right), \quad \forall \boldsymbol{v} \in \boldsymbol{V}_{\mathcal{T}}, \tag{2.10}$$

where $\delta_x^2(\boldsymbol{v}, \boldsymbol{\zeta}) = v_x(\boldsymbol{\zeta}) - (\mathcal{I}_{\mathcal{T}}^0 \boldsymbol{v})_x(\boldsymbol{\zeta})$ *and* $\delta_y^2(\boldsymbol{v}, \boldsymbol{\zeta}) = v_y(\boldsymbol{\zeta}) - (\mathcal{I}_{\mathcal{T}}^0 \boldsymbol{v})_y(\boldsymbol{\zeta})$.

Proof. By construction, for each $E \in \mathcal{T}$, it holds

$$\boldsymbol{\mu}_p^{\mathrm{div}}(\mathcal{I}_E \boldsymbol{v}, E) = \boldsymbol{\mu}_p^{\mathrm{div}}(\boldsymbol{v}, E) = \boldsymbol{\mu}_p^{\mathrm{div}}(\mathcal{I}_{\mathcal{T}}^0 \boldsymbol{v}, E) \text{ for } 1 \le p \le k-2,$$

and

$$\boldsymbol{\mu}_p^{\perp}(\mathcal{I}_E \boldsymbol{v}, E) = \boldsymbol{\mu}_p^{\perp}(\boldsymbol{v}, E) = \boldsymbol{\mu}_p^{\perp}(\mathcal{I}_{\mathcal{T}}^0 \boldsymbol{v}, E) \text{ for } 0 \le p \le k-4.$$

This implies that $\boldsymbol{\mu}_p^{\mathrm{div}}(\mathcal{I}_E \boldsymbol{v} - \mathcal{I}_{\mathcal{T}}^0 \boldsymbol{v}, E) = \boldsymbol{0}$ for $1 \le p \le k-2$ and $\boldsymbol{\mu}_p^{\perp}(\mathcal{I}_E \boldsymbol{v} - \mathcal{I}_{\mathcal{T}}^0 \boldsymbol{v}, E) = \boldsymbol{0}$ for $0 \le p \le k-4$. Recalling that $\boldsymbol{v}(\mathbf{x}) = (\mathcal{I}_E \boldsymbol{v})(\mathbf{x})$ for $\boldsymbol{x} \in \mathcal{P}_E$, we write

$$|\mathcal{I}_E \boldsymbol{v} - \mathcal{I}_{\mathcal{T}}^0 \boldsymbol{v}|_{1,E^2} \simeq \sum_{\boldsymbol{x} \in \mathcal{P}_E} \left| (\mathcal{I}_E \boldsymbol{v} - \mathcal{I}_{\mathcal{T}}^0 \boldsymbol{v})(\boldsymbol{x}) \right|^2 = \sum_{\boldsymbol{x} \in \mathcal{P}_E} \left| (\boldsymbol{v} - \mathcal{I}_{\mathcal{T}}^0 \boldsymbol{v})(\boldsymbol{x}) \right|^2.$$

Summing on all the triangles, we obtain

$$\sum_{E \in \mathcal{T}} |\mathcal{I}_E \boldsymbol{v} - \mathcal{I}_{\mathcal{T}}^0 \boldsymbol{v}|_{1,E^2} \simeq \sum_{\boldsymbol{x} \in \mathcal{N}} \left| (\boldsymbol{v} - \mathcal{I}_{\mathcal{T}}^0 \boldsymbol{v})(\boldsymbol{x}) \right|^2 = \sum_{\boldsymbol{x} \in \mathcal{H}} \left| (\boldsymbol{v} - \mathcal{I}_{\mathcal{T}}^0 \boldsymbol{v})(\boldsymbol{x}) \right|^2.$$

Where in the last equality we used $\boldsymbol{v}(\mathbf{x}) = (\mathcal{I}_{\mathcal{T}}^0 \boldsymbol{v})(\mathbf{x})$ for $\boldsymbol{x} \in \mathcal{P}$. □

The two lemmas allow us to give one last result about the interpolation operators.

Proposition 2. *Let $\mathcal{T}$ be Λ-admissible. Then, there exists a constant $C_I > 0$, depending on Λ, but independent of $\mathcal{T}$, such that*

$$|\boldsymbol{v} - \mathcal{I}_{\mathcal{T}}^0 \boldsymbol{v}|_{1,\Omega} \le C_I |\boldsymbol{v} - \mathcal{I}_{\mathcal{T}} \boldsymbol{v}|_{1,\mathcal{T}} \quad \forall \boldsymbol{v} \in \boldsymbol{V}_{\mathcal{T}}. \tag{2.11}$$

Proof. By the triangular inequality:

$$|\boldsymbol{v} - \mathcal{I}_{\mathcal{T}}^0 \boldsymbol{v}|_{1,\Omega} \le |\boldsymbol{v} - \mathcal{I}_{\mathcal{T}} \boldsymbol{v}|_{1,\mathcal{T}} + |\mathcal{I}_{\mathcal{T}} \boldsymbol{v} - \mathcal{I}_{\mathcal{T}}^0 \boldsymbol{v}|_{1,\mathcal{T}}, \tag{2.12}$$

To simplify the notation we consider the vectors

$$\boldsymbol{\delta}_x = (\delta_x(\boldsymbol{v}, \boldsymbol{\zeta}))_{\boldsymbol{\zeta} \in \mathcal{H}}, \qquad \boldsymbol{\delta}_y = (\delta_y(\boldsymbol{v}, \boldsymbol{\zeta}))_{\boldsymbol{\zeta} \in \mathcal{H}},$$

and

$$\boldsymbol{d}_x = (d_x(\boldsymbol{v}, \boldsymbol{\zeta}))_{\zeta \in \mathcal{H}}, \qquad \boldsymbol{d}_y = (d_y(\boldsymbol{v}, \boldsymbol{\zeta}))_{\zeta \in \mathcal{H}}.$$

In (2.12), using (2.10), the second term in the right hand side is bounded by $\|\boldsymbol{\delta}_x\|^2_{l^2(\mathcal{H})} + \|\boldsymbol{\delta}_y\|^2_{l^2(\mathcal{H})}$. If we can show that

$$\|\boldsymbol{\delta}_x\|^2_{l^2(\mathcal{H})} \lesssim \|\boldsymbol{d}_x\|^2_{l^2(\mathcal{H})},$$

and

$$\|\boldsymbol{\delta}_y\|^2_{l^2(\mathcal{H})} \lesssim \|\boldsymbol{d}_y\|^2_{l^2(\mathcal{H})},$$

then the result follows as a consequence of (2.9). To this end, consider $\boldsymbol{\zeta} \in \mathcal{H}$ that is generated as a level of refinement j of an edge L. We repeat the construction involved at the beginning of this section, so that $\boldsymbol{\zeta} = \boldsymbol{\zeta}_i$ for some $1 \leq i \leq k$ and some sub-edge of L. We write $(v_x^*, v_y^*) = \boldsymbol{v}^* := \mathcal{I}_{\mathcal{T}}^0 \boldsymbol{v}$ for short.

$$\begin{aligned}
\delta_x(\boldsymbol{\zeta}_i) &= v_x(\boldsymbol{\zeta}_i) - v_x^*(\boldsymbol{\zeta}_i) = v_x(\boldsymbol{\zeta}_i) - \sum_{n=1}^{k+1} \alpha_{i,n} v_x^*(\boldsymbol{\xi}_n) \\
&= v_x(\boldsymbol{\zeta}_i) - \sum_{n=1}^{k+1} \alpha_{i,n} v_x(\boldsymbol{\xi}_n) - \sum_{n=1}^{k+1} \alpha_{i,n} \left(v_x^*(\boldsymbol{\xi}_n) - v_x(\boldsymbol{\xi}_n)\right) \\
&= d_x(\boldsymbol{\zeta}_i) + \sum_{n=1}^{k+1} \alpha_{i,n} \delta_x(\boldsymbol{\xi}_n)
\end{aligned}$$

This computation can be repeated in a recursive way, and recalling that $\delta_x(\boldsymbol{\xi}_n) = 0$ if $\boldsymbol{\xi}_n$ is a proper node, we get a matrix $\mathbf{W} : l^2(\mathcal{H}) \to l^2(\mathcal{H})$ such that $\boldsymbol{\delta}_x = \mathbf{W}\boldsymbol{d}_x$. Since $\mathbf{W}$ only depends on the positions of the hanging nodes, the same procedure applied to the details of the y components gives $\boldsymbol{\delta}_y = \mathbf{W}\boldsymbol{d}_y$. Thus, it is sufficient to show

$$\|\mathbf{W}\|_2 \lesssim 1.$$

Continuation of the proof is the exact same as [9]. □

2.3 Upper bound for the stabilization term

We state the following result

Proposition 3. *Let $(\boldsymbol{u}_{\mathcal{T}}, p_{\mathcal{T}})$ be the solution of (1.24). There exists a constant $C_B > 0$ independent of $\mathcal{T}$, $\boldsymbol{u}_{\mathcal{T}}$ and γ, such that*

$$\gamma^2 S_{\mathcal{T}}(\boldsymbol{u}_{\mathcal{T}}, \boldsymbol{u}_{\mathcal{T}}) \leq C_B \eta_{\mathcal{T}}^2(\boldsymbol{u}_{\mathcal{T}}, p_{\mathcal{T}}). \tag{2.13}$$

Proof. From the first equation in (1.24), for every $\boldsymbol{w} \in \boldsymbol{V}_{\mathcal{T}}^0$

$$\begin{aligned}
\gamma S_{\mathcal{T}}(\boldsymbol{u}_{\mathcal{T}}, \boldsymbol{u}_{\mathcal{T}}) &= \gamma S_{\mathcal{T}}(\boldsymbol{u}_{\mathcal{T}}, \boldsymbol{u}_{\mathcal{T}} - \boldsymbol{w}) \\
&= \mathcal{F}_{\mathcal{T}}(\boldsymbol{u}_{\mathcal{T}} - \boldsymbol{w}) - a_{\mathcal{T}}(\boldsymbol{u}_{\mathcal{T}}, \boldsymbol{u}_{\mathcal{T}} - \boldsymbol{w}) - b(\boldsymbol{u}_{\mathcal{T}} - \boldsymbol{w}, p_{\mathcal{T}}).
\end{aligned}$$

We write $\boldsymbol{e}_{\mathcal{T}} := \boldsymbol{u}_{\mathcal{T}} - \boldsymbol{w}$, then

$$\gamma S_{\mathcal{T}}(\boldsymbol{u}_{\mathcal{T}}, \boldsymbol{u}_{\mathcal{T}}) = \sum_{E\in\mathcal{T}} \left(\int_E \boldsymbol{f}_{\mathcal{T}} \cdot \boldsymbol{e}_{\mathcal{T}} - \int_E \nu\nabla\left(\Pi_k^{\nabla,E}\boldsymbol{u}_{\mathcal{T}}\right) : \nabla\left(\Pi_k^{\nabla,E}\boldsymbol{e}_{\mathcal{T}}\right) - \int_E (\nabla\cdot\boldsymbol{e}_{\mathcal{T}})p_{\mathcal{T}} \right). \tag{2.14}$$

Now consider the second integral in the right hand side of (2.14). By definition of $\Pi_k^{\nabla,E}$ and then integrating by part, we get

$$\begin{aligned} -\int_E \nu\nabla\left(\Pi_k^{\nabla,E}\boldsymbol{u}_{\mathcal{T}}\right) : \nabla\left(\Pi_k^{\nabla,E}\boldsymbol{e}_{\mathcal{T}}\right) &= -\int_E \nu\nabla\left(\Pi_k^{\nabla,E}\boldsymbol{u}_{\mathcal{T}}\right) : \nabla\boldsymbol{e}_{\mathcal{T}} \\ &= -\int_{\partial E} \nu\nabla\left(\Pi_k^{\nabla,E}\boldsymbol{u}_{\mathcal{T}}\right)\boldsymbol{n}\cdot\boldsymbol{e}_{\mathcal{T}} + \int_E \nu\Delta\left(\Pi_k^{\nabla,E}\boldsymbol{u}_{\mathcal{T}}\right)\cdot\nabla\boldsymbol{e}_{\mathcal{T}}, \end{aligned} \tag{2.15}$$

whereas, by integrating by parts the last integral, we get

$$-\int_E (\nabla\cdot\boldsymbol{e}_{\mathcal{T}})p_{\mathcal{T}} = -\int_{\partial E} \boldsymbol{e}_{\mathcal{T}}\cdot\boldsymbol{n}p_{\mathcal{T}} + \int_E \nabla p_{\mathcal{T}}\cdot\boldsymbol{e}_{\mathcal{T}}. \tag{2.16}$$

Substituting (2.15) and (2.16) into (2.14), we obtain

$$\begin{aligned} \gamma S_{\mathcal{T}}(\boldsymbol{u}_{\mathcal{T}}, \boldsymbol{u}_{\mathcal{T}}) &= \sum_{E\in\mathcal{T}} \left(\int_E \left(\boldsymbol{f}_{\mathcal{T}} + \nu\Delta\Pi_k^{\nabla,E}\boldsymbol{u}_{\mathcal{T}} + \nabla p_{\mathcal{T}}\right)\cdot\boldsymbol{e}_{\mathcal{T}} - \int_{\partial E}\left(\nu\nabla\Pi_k^{\nabla,E}\boldsymbol{u}_{\mathcal{T}} + p_{\mathcal{T}}\mathbf{I}\right)\boldsymbol{n}\cdot\boldsymbol{e}_{\mathcal{T}} \right) \\ &\leq \sum_{E\in\mathcal{T}} \left(h_E\|\boldsymbol{r}_{\mathcal{T}}(E;\boldsymbol{u}_{\mathcal{T}},p_{\mathcal{T}})\|_{0,E}h_E^{-1}\|\boldsymbol{e}_{\mathcal{T}}\|_{0,E} + \frac{1}{2}\sum_{e\in\mathcal{E}_E} h_E^{\frac{1}{2}}\|\boldsymbol{j}_{\mathcal{T}}(e;\boldsymbol{u}_{\mathcal{T}},p_{\mathcal{T}})\|_{0,e}h_E^{-\frac{1}{2}}\|\boldsymbol{e}_{\mathcal{T}}\|_{0,e} \right) \end{aligned}$$

Now, following the same strategy as [9], for any $\delta > 0$, it holds

$$\gamma S_{\mathcal{T}}(\boldsymbol{u}_{\mathcal{T}}, \boldsymbol{u}_{\mathcal{T}}) \leq \frac{1}{2\delta}\eta_{\mathcal{T}}^2(\boldsymbol{u}_{\mathcal{T}}, p_{\mathcal{T}}) + \frac{\delta}{2}\Phi_{\mathcal{T}}(\boldsymbol{e}_{\mathcal{T}}), \tag{2.17}$$

where

$$\Phi_{\mathcal{T}}(\boldsymbol{e}_{\mathcal{T}}) = \sum_{E\in\mathcal{T}} \left(h_E^{-2}\|\boldsymbol{e}_{\mathcal{T}}\|_{0,E}^2 + \frac{1}{2}\sum_{e\in\mathcal{E}_E} h_E^{-1}\|\boldsymbol{e}_{\mathcal{T}}\|_{0,e}^2 \right).$$

We choose $\boldsymbol{w} = \mathcal{I}_{\mathcal{T}}^0\boldsymbol{u}_{\mathcal{T}}$ and applying (2.4) and (1.36), we get

$$\Phi_{\mathcal{T}}(\boldsymbol{u}_{\mathcal{T}} - \mathcal{I}_{\mathcal{T}}^0\boldsymbol{u}_{\mathcal{T}}) \lesssim |\boldsymbol{u}_{\mathcal{T}} - \mathcal{I}_{\mathcal{T}}^0\boldsymbol{u}_{\mathcal{T}}|_{1,\Omega} \lesssim |\boldsymbol{u}_{\mathcal{T}} - \mathcal{I}_{\mathcal{T}}\boldsymbol{u}_{\mathcal{T}}|_{1,\Omega} \simeq \gamma S_{\mathcal{T}}(\boldsymbol{u}_{\mathcal{T}}, \boldsymbol{u}_{\mathcal{T}}),$$

i.e. there exists a constant $C_B > 0$ such that

$$\Phi_{\mathcal{T}}(\boldsymbol{u}_{\mathcal{T}} - \mathcal{I}_{\mathcal{T}}^0\boldsymbol{u}_{\mathcal{T}}) \leq C_B S_{\mathcal{T}}(\boldsymbol{u}_{\mathcal{T}}, \boldsymbol{u}_{\mathcal{T}}). \tag{2.18}$$

Substituting (2.18) in (2.17) and choosing $\delta = \frac{\gamma}{C_B}$, we obtain

$$\gamma^2 S_{\mathcal{T}}(\boldsymbol{u}_{\mathcal{T}}, \boldsymbol{u}_{\mathcal{T}}) \leq C_B\eta_{\mathcal{T}}^2(\boldsymbol{u}_{\mathcal{T}}, p_{\mathcal{T}}).$$

□

Combining (1.36) and (2.13) we obtain the following result:

Corollary 1. *It holds*

$$|\boldsymbol{u} - \boldsymbol{u}_{\mathcal{T}}|_{1,\Omega}^2 + \|p - p_{\mathcal{T}}\|_{1,\Omega}^2 \leq C_U\eta_{\mathcal{T}}^2(\boldsymbol{u}_{\mathcal{T}}, p_{\mathcal{T}}) + C_{apost}\mathcal{F}^2, \tag{2.19}$$

where $C_U = C_{apost}\left(1 + \frac{C_B}{\gamma^2}\right)$.

Chapter 3

Numerical Results

In this chapter, we validate the performance of the proposed method and the reliability of the a posteriori error estimator through a series of numerical tests. We consider a problem with known analytical solutions in order to verify the validity of the results obtained in chapter 2. The problem we propose is test 6.1 from [11], where $\boldsymbol{f}$ is chosen in such a way that the continuous solution of the problem is

$$\boldsymbol{u}(x,y) = \begin{pmatrix} -\frac{1}{2}\cos^2(x)\sin(y)\cos(y) \\ \frac{1}{2}\cos^2(y)\sin(x)\cos(x) \end{pmatrix}, \qquad p(x,y) = \sin(x) - \sin(y). \tag{3.1}$$

We set $\nu = 1$ and $\gamma = 1$. The domain of the problem is the square $[0,1]^2 \subset \mathbb{R}^2$. The figures show the total error

$$\varepsilon_{tot}(\boldsymbol{u}_\mathcal{T}, p_\mathcal{T}) := (\|\nabla \boldsymbol{u} - \Pi_{k-1}^{0,E} \nabla \boldsymbol{u}_\mathcal{T}\|_{0,\Omega}^2 + \|p - p_\mathcal{T}\|_{0,\Omega}^2)^{\frac{1}{2}},$$

as well as the quantities $\eta_\mathcal{T}(\boldsymbol{u}_\mathcal{T}, p_\mathcal{T})$, $S_\mathcal{T}(\boldsymbol{u}_\mathcal{T}, \boldsymbol{u}_\mathcal{T})$ and $(\eta_\mathcal{T}(\boldsymbol{u}_\mathcal{T}, p_\mathcal{T})^2 + S_\mathcal{T}(\boldsymbol{u}_\mathcal{T}, \boldsymbol{u}_\mathcal{T})^2)^{\frac{1}{2}}$. For short, we define

$$\eta_\mathcal{T}^*(\boldsymbol{u}_\mathcal{T}, p_\mathcal{T}) = \left(\eta_\mathcal{T}(\boldsymbol{u}_\mathcal{T}, p_\mathcal{T})^2 + S_\mathcal{T}(\boldsymbol{u}_\mathcal{T}, \boldsymbol{u}_\mathcal{T})^2\right)^{\frac{1}{2}}.$$

Vem order $k = 2$ and $k = 3$ are considered.

3.1 Test 1

The problem (3.1) is solved on four triangular meshes with aligned edges, with increasing number of degrees of freedom. The meshes are shown in Figures 3.1 and 3.2. The result of the simulation is shown in Figure 3.3. We can observe that all the values in the plots have the same scaling coefficient, that is around $-(N_{dofs})^{\frac{k}{2}}$. This is coherent with the a priori estimates (1.28) and (1.29) and the a posteriori estimates (1.36) (2.19). The stabilization-free upper bound and the standard upper bound are very close to each other, as the stabilization term is much lower compared to the total error.

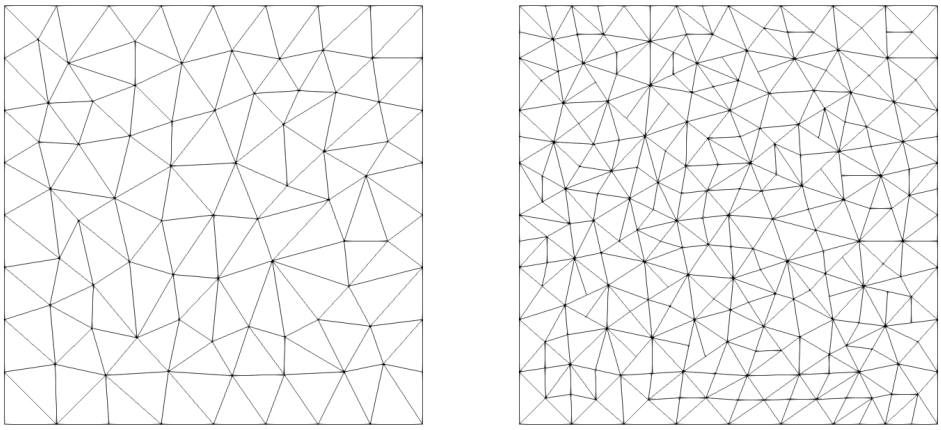

Figure 3.1. Initial mesh with no aligned edges on the right. First refined mesh on the left

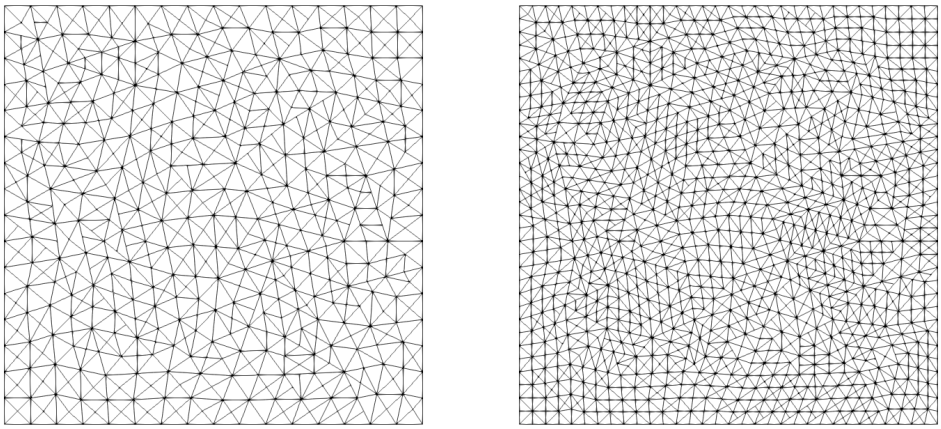

Figure 3.2. Second refined mesh on the right. Third refined mesh on the left

3.2 Test 2

As a further investigation, the problem (3.1) is solved on three different sequences of homogeneous meshes, including triangular, square, and Voronoi polygonal meshes. Examples of each mesh are shown in Figure 3.4. For each mesh, various VEM simulations of the problem have been run, with the maximum area of the elements halving in each simulation (so that the number of degrees of freedom N_{dofs} approximately doubles). Specifically, every sequence of meshes is generated by maximum area parameters of $\{0.01, 0.005, 0.0025, 0.00125\}$. The result of the simulations is shown in Figures 3.5 (triangular), 3.6(square), and 3.7(polygonal). According to the theoretical results, and similarly to the Test 1, presented in (1.28), (1.29) and (1.36), the total error and the global a posteriori estimator scale as $h^k \approx N_{dofs}^{-k/2}$. The stabilization term represents a

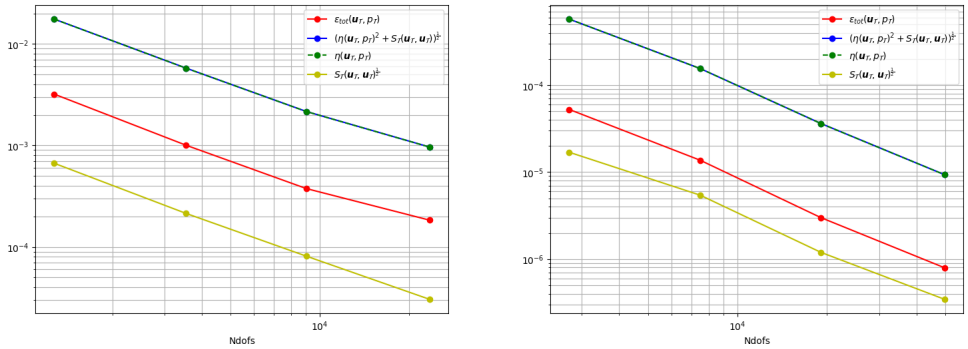

Figure 3.3. Results of (3.1) on triangular mesh with aligned edges, order $k = 2$ (left) and $k = 3$ (right).

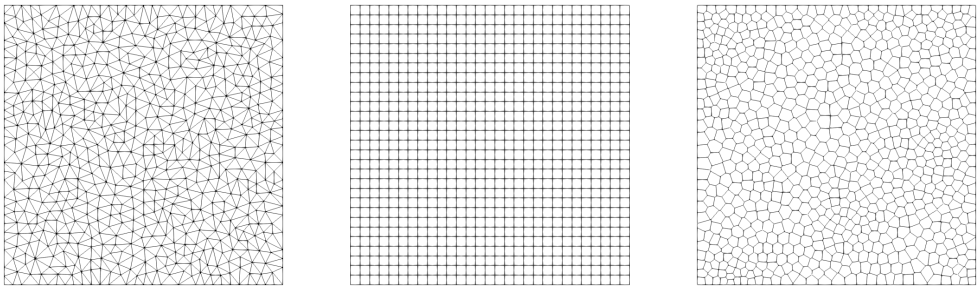

Figure 3.4. Examples of the three types of meshes: triangular(left), square(center), polygonal(right). Each mesh has maximum area parameter set as 1/800.

small contribution to the estimator. This can be seen in the figures as the upper bounds η and η_* are very close to each other.

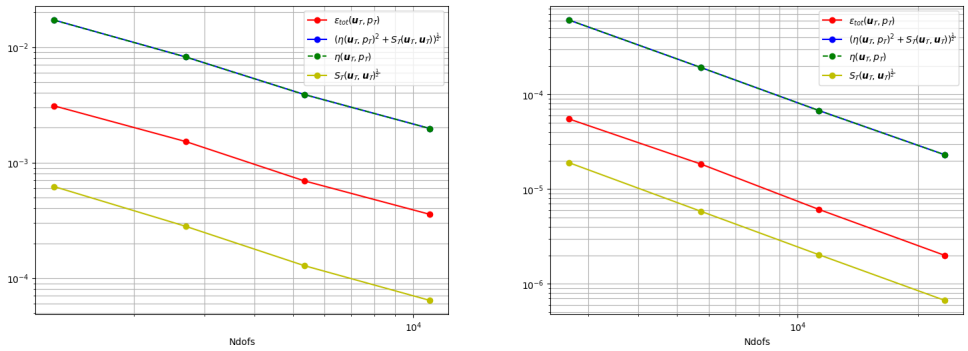

Figure 3.5. Results of (3.1) on homogeneous triangular mesh, order $k = 2$ (left) and $k = 3$ (right).

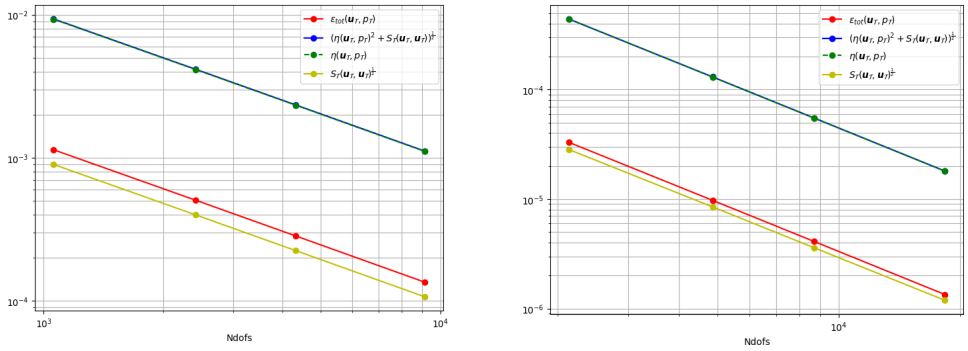

Figure 3.6. Results of (3.1) on homogeneous square mesh, order $k = 2$ (left) and $k = 3$ (right).

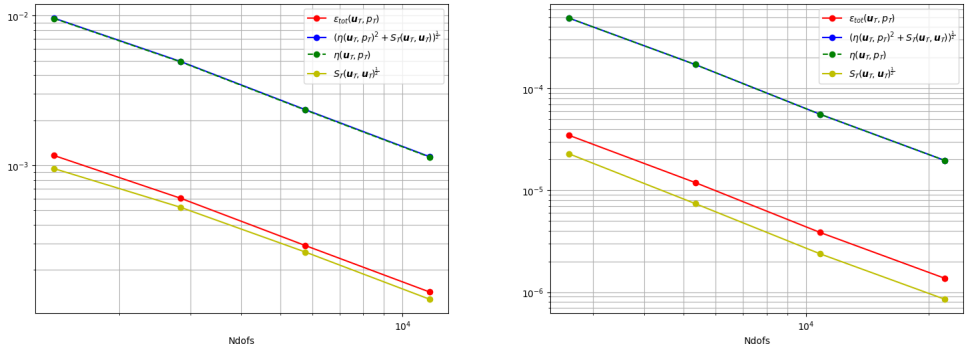

Figure 3.7. Results of (3.1) on homogeneous polygonal mesh, order $k = 2$ (left) and $k = 3$ (right).

Appendix A

Implementation

In this section, we focus on the implementation of the a posteriori estimator introduced in the previous chapter. We start the first section by pointing out the libraries involved to assemble the discrete problem. Then, we define some basic elements needed to compute the quantities defined in 1.2, which will be used in the computation of the estimator.

A.1 Libraries and code basics

The numerical results presented in this thesis have been obtained using a code developed in C++. This section outlines the basics of the code. These basics, as well as the assembling and solving of the system, and the computation of the errors, are already implemented in the GeDiM [6] and PolyDiM [7] libraries. Specifically, the GeDiM library manages the discretization of the domain, the quadrature rules, the solution of the assembled linear system and many utility functions such as the solution export. The PolyDiM library handles the tasks that are related to the specific problem, including the management of the problem data and of VEM spaces, the assembling of the system and the computation of the errors. The libraries and the implemented code rely on the Eigen library [14] to store the variables and to make linear algebra operations. Creation of the mesh is done through the Voro++ library [15], while post processing and plotting are done both in Paraview and Python.

Now, we describe the fundamental vectors and matrices that are implemented in the PolyDiM and GeDiM libraries that will be involved in the computation of the a posteriori estimator From now on, we denote with N_k the dimension of the space $\mathbb{P}_k(E)$. We want to establish a unique indexing for all possible multi-indices. We choose

$$n(\boldsymbol{\alpha}) = 1 + \alpha_y + \frac{(\alpha_x + \alpha_y)\alpha_x + \alpha_y + 1}{2}. \tag{A.1}$$

Since we have to compute quantities defined by integrals, we need to choose a quadrature rule. The GeDiM library implements, on an element E, the Gauss-Lobatto quadrature rule, allowing us to compute exact polynomial integrals up to order $2k$, with k being the VEM order. Thus, we have N_q^E quadrature points and weights, stored in $\{\boldsymbol{x}_i^E\}_{i=1}^{N_q^E}$ and

$\mathbf{w}^E \in \mathbb{R}^{N_q^E}$, respectively. We define the Vandermonde matrix of order k, $\boldsymbol{\mathcal{V}}_k^E \in \mathbb{R}^{N_q^E \times N_k}$

$$(\boldsymbol{\mathcal{V}}_k^E)_{ij} = m_j(\boldsymbol{x}_i) \quad i = 1, ..., N_q^E \; j = 1, ..., N_k \tag{A.2}$$

where m_j is the j-th element of the basis $\mathcal{M}_k(E)$, according to the indexing previously defined. The Vandermonde matrix is useful for evaluating a polynomial $q_k \in \mathbb{P}_k(E)$ on the quadrature points. Let $\mathbf{p} \in \mathbb{R}^{N_k}$ be the vector of monomial coefficients of q_k. Then, the vector $\tilde{\mathbf{p}} \in \mathbb{R}^{N_q^E}$, defined by

$$\tilde{\mathbf{p}} = \boldsymbol{\mathcal{V}}_k^E \mathbf{p} \tag{A.3}$$

has in the i-th component the polynomial q_k evaluated in the i-th quadrature point.

We proceed by defining the matrices needed to compute polynomial derivatives. First, notice that the derivatives of the monomial m_j, with $j = n(\boldsymbol{\alpha})$ for some $\boldsymbol{\alpha}$, is a multiple of another monomial:

$$\frac{\partial m_j}{\partial x} = \frac{\alpha_x}{h_E} m_i \quad i = j - \alpha_x - \alpha_y \text{ if } \alpha_x > 0, \tag{A.4}$$

$$\frac{\partial m_j}{\partial y} = \frac{\alpha_y}{h_E} m_i \quad i = j - \alpha_x - \alpha_y - 1 \text{ if } \alpha_y > 0, \tag{A.5}$$

the derivatives are null, otherwise. The previous relationships can be written in a vector form by defining two matrices $\mathbf{D}_{k,x}^E$, and $\mathbf{D}_{k,y}^E \in \mathbb{R}^{N_k \times N_k}$ such that:

$$(\mathbf{D}_{k,x}^E)_{ij} = \begin{cases} \frac{\alpha_x}{h_E} & \text{if } i = j - \alpha_x - \alpha_y \\ 0 & \text{otherwise} \end{cases},$$

and

$$(\mathbf{D}_{k,y}^E)_{ij} = \begin{cases} \frac{\alpha_y}{h_E} & \text{if } i = j - \alpha_x - \alpha_y - 1 \\ 0 & \text{otherwise} \end{cases}.$$

The two matrices allow us to represent the derivatives of a polynomial $q_k \in \mathbb{P}_k(E)$, $\frac{\partial q_k}{\partial x}$ and $\frac{\partial q_k}{\partial x}$ with respect to the base $\mathcal{M}_k(R)$ by computing:

$$\mathbf{p}_x := \mathbf{D}_{k,x}^E \mathbf{p},$$
$$\mathbf{p}_y := \mathbf{D}_{k,y}^E \mathbf{p},$$

whereas their evaluation in the quadrature points, which we denote by $\tilde{\mathbf{p}}_x$ and $\tilde{\mathbf{p}}_y$, respectively, is obtained by multiplying their monomial representation by the Vandermonde matrix $\boldsymbol{\mathcal{V}}_k^E$.

Finally, we need to compute the laplacian of a polynomial. We can define the laplacian matrix

$$\mathbf{L}_k^E = (\mathbf{D}_{k,x}^E)^2 + (\mathbf{D}_{k,y}^E)^2. \tag{A.6}$$

The laplacian matrix allows us to compute the coefficients of the laplacian of a polynomial, as well as its evaluation in quadrature points in the same way as the derivative matrices.

Since we want to compute edge derivatives, we define on an edge $e \in \mathcal{E}_E$ both a set of N_q^e quadrature points and a set of N_q^e quadrature weights. Those sets are denoted

by $\{\boldsymbol{x}_i^e\}_{i=1}^{N_q^e}$ and $\mathbf{w}^E \in \mathbb{R}^{N_q^e}$, respectively. Then, we define the edge Vandermonde matrix $\boldsymbol{\mathcal{V}}_k^e \in \mathbb{R}^{N_q^e} \times \mathbb{R}^{N_k}$ defined by

$$(\boldsymbol{\mathcal{V}}_k^e)_{ij} = m_j(\boldsymbol{x}_i^e) \quad i = 1, ..., N_q^e \; j = 1, ..., N_k.$$

We define a basis for the local velocity space as follows

- The $2kn_E$ basis functions of the edges $\boldsymbol{\varphi}_{i,x}^{\partial}$ and $\boldsymbol{\varphi}_{i,y}^{\partial}$ as

$$\begin{cases} \boldsymbol{\varphi}_{i,x}^{\partial}(\boldsymbol{x}_j^{\partial E}) = \begin{pmatrix} \delta_{i,j} \\ 0 \end{pmatrix} & j = 1, ..., kn_E, \\ \int_E \nabla \cdot \boldsymbol{\varphi}_{i,x}^{\partial} m_j = 0 & j = 2, ..., N_{k-1}, \\ \int_E \boldsymbol{x}^{\perp} \cdot \boldsymbol{\varphi}_{i,x}^{\partial} m_j = 0 & j = 1, ..., N_{k-3}, \end{cases}$$

  and

$$\begin{cases} \boldsymbol{\varphi}_{i,y}^{\partial}(\boldsymbol{x}_j^{\partial E}) = \begin{pmatrix} 0 \\ \delta_{i,j} \end{pmatrix} & j = 1, ..., kn_E, \\ \int_E \nabla \cdot \boldsymbol{\varphi}_{i,y}^{\partial} m_j = 0 & j = 2, ..., N_{k-1}, \\ \int_E \boldsymbol{x}^{\perp} \cdot \boldsymbol{\varphi}_{i,y}^{\partial} m_j = 0 & j = 1, ..., N_{k-3}; \end{cases}$$

- the $N_{k-1} - 1$ for the divergence $\boldsymbol{\varphi}_i^{\mathrm{div}}$

$$\begin{cases} \boldsymbol{\varphi}_i^{\mathrm{div}}(\boldsymbol{x}_j^{\partial E}) = \mathbf{0} & j = 1, ..., kn_E, \\ \int_E \nabla \cdot \boldsymbol{\varphi}_i^{\mathrm{div}} m_j = \delta_{i,j} & j = 2, ..., N_{k-1}, \\ \int_E \boldsymbol{x}^{\perp} \cdot \boldsymbol{\varphi}_i^{\mathrm{div}} m_j = 0 & j = 1, ..., N_{k-3}; \end{cases}$$

- the $N_{k-1} - 1$ for the divergence $\boldsymbol{\varphi}_i^{\perp}$

$$\begin{cases} \boldsymbol{\varphi}_i^{\perp}(\boldsymbol{x}_j^{\partial E}) = \mathbf{0} & j = 1, ..., kn_E, \\ \int_E \nabla \cdot \boldsymbol{\varphi}_i^{\perp} m_j = 0 & j = 2, ..., N_{k-1}, \\ \int_E \boldsymbol{x}^{\perp} \cdot \boldsymbol{\varphi}_i^{\perp} m_j = \delta_{i.j} & j = 1, ..., N_{k-3}. \end{cases}$$

Each of the projector operators $\Pi_k^{\nabla,E}$ and $\nabla\Pi_k^{0,E}$ is implemented as two matrices representing the two components of the projected velocity. Thus, we have the matrices $\boldsymbol{\Pi}_{k,x}^{\nabla,E}, \boldsymbol{\Pi}_{k,y}^{\nabla,E}, \boldsymbol{\Pi}_{k,x}^{0,E}, \boldsymbol{\Pi}_{k,y}^{0,E} \in \mathbb{R}^{N_k \times \dim(\boldsymbol{V}_k^E)}$, defined by

$$\mathrm{dof}_{\mathbb{P}_k(E)} \left(\Pi_k^{\nabla,E} \boldsymbol{v}\right)_* = \boldsymbol{\Pi}_{k,*}^{\nabla,E} \mathrm{dof}_{\boldsymbol{V}_k^E}(\boldsymbol{v}) \quad \forall \boldsymbol{v} \in \boldsymbol{V}_k^E, * \in \{x, y\},$$

and

$$\mathrm{dof}_{\mathbb{P}_k(E)} \left(\Pi_k^{0,E} \boldsymbol{v}\right)_* = \boldsymbol{\Pi}_{k,*}^{0,E} \mathrm{dof}_{\boldsymbol{V}_k^E}(\boldsymbol{v}) \quad \forall \boldsymbol{v} \in \boldsymbol{V}_k^E, * \in \{x, y\},$$

where $\mathrm{dof}_{\mathbb{P}_k(E)}$ is the vector of the coefficients of a polynomial with respect to the monomial basis and $\mathrm{dof}_{\boldsymbol{V}_k^E}$ is the vector of the coefficients of a velocity with respect to the velocity basis.

A.2 A posteriori estimator implementation

A.2.1 Source term projection

To compute the internal residual term of (1.30), we need to compute $\boldsymbol{f}_{\mathcal{T}}$ and evaluate it in quadrature points. The issue is that $\boldsymbol{f}$ is not an element of $\boldsymbol{V}_k^E$. Thus, we cannot represent it in the degrees of freedom of the local velocity space. Since each component of $\Pi_k^{0,E}\boldsymbol{f}$ is a polynomial, we can represent it with respect to the basis $\mathcal{M}_k(E)$. Let $\mathbf{f}_{\mathcal{T},x}$ and $\mathbf{f}_{\mathcal{T},y}$ be the vectors containing monomial coefficients of each component of the projected source term. We write

$$\Pi_k^{0,E} f_x = \sum_{j=1}^{N_k} (\mathbf{f}_{\mathcal{T},x})_j m_j,$$

and

$$\Pi_k^{0,E} f_y = \sum_{j=1}^{N_k} (\mathbf{f}_{\mathcal{T},y})_j m_j.$$

We recall the definition (1.12) of $\Pi_k^{0,E}$ and notice that it holds for the elements of the basis $\mathcal{M}_k(E)$

$$\begin{aligned}
(\Pi_k^{0,E} f_*, m_i)_E &= (f_*, m_i)_E \quad i = 1, ..., N_k,\ * \in \{x, y\}, \\
\left(\sum_{j=1}^{N_k} (\mathbf{f}_{\mathcal{T},*})_j m_j, m_i \right)_E &= (f_*, m_i)_E \quad i = 1, ..., N_k,\ * \in \{x, y\}, \\
\sum_{j=1}^{N_k} (\mathbf{H}^E)_{ij} (\mathbf{f}_{\mathcal{T},*})_j &= (f_*, m_i)_E \quad i = 1, ..., N_k,\ * \in \{x, y\}.
\end{aligned}$$

Where $(\mathbf{H}^E)_{ij} := (m_j, m_i)_E$ defines the mass matrix of the basis $\mathcal{M}_k(E)$. The matrix $\mathbf{H}^E$ is symmetric and positive definite, and it is computable as shown below

$$\mathbf{H}^E = (\boldsymbol{\mathcal{V}}_k^E)^T \mathbf{W}^E \boldsymbol{\mathcal{V}}_k^E.$$

The integrals in the right hand side of the above equation are defined and computable as well. Let $\tilde{\mathbf{f}}_x, \tilde{\mathbf{f}}_y \in \mathbb{R}^{N_q^E}$ denote the values of f_x and f_y, respectively, evaluated in the quadrature points.

$$(f_*, m_i) = (\boldsymbol{\mathcal{V}}_k^E)_i^T \mathbf{W}^E \tilde{\mathbf{f}}_*,$$

where $(\boldsymbol{\mathcal{V}}_k^E)_i^T$ is the i-th column of the Vandermonde matrix. The vectors $\mathbf{f}_{\mathcal{T},x}$ and $\mathbf{f}_{\mathcal{T},y}$ are obtained by solving two linear systems.

A.2.2 Computation of local estimator components

We show in a detailed way how the quantities defined in chapter 1.3.1 have been computed. First, we establish some notation that will be used for the rest of this chapter. For an element $E \in \mathcal{T}$, the vectors $\mathbf{u}_{\mathcal{T}}^E \in \mathbb{R}^{\dim(\boldsymbol{V}_{\mathcal{T}}^E)}$ and $\mathbf{p}_{\mathcal{T}}^E \in \mathbb{R}^{N_{k-1}}$ represent the components, with respect of their basis, of the local solutions of velocity and pressure, respectively. For a generic vector $\mathbf{a}$, we denote by $\mathbf{a}^2$ the vector containing each component of $\mathbf{a}$ squared.

Most of the quantities we want to compute have a computational complexity of the number of triangular shaped elements $|\mathcal{T}|$. The only exception to this is the jump term of the edges, which has a complexity of twice the number of internal edges. Moreover, the latter term requires to have uploaded two local space objects at the same time. Local space objects are structures that contain the geometrical information of the element E as well as the Vandermonde matrices and the projection matrices of that elements. Each time a local space object is created, the matrices are computed. Thus, we want to load local spaces the least times possible. For this reason, all computations happen inside a loop over the elements, which contains a cycle on the edges of the element to compute jump terms.

The first term we compute is (1.30). For the first contribution, being the norm of the residual given by the projected solution, we define the internal residual vectors $\mathbf{r}_x^E, \mathbf{r}_y^E \in \mathbb{R}^{N_q^E}$, whose components contain the residual evaluated in quadrature points.

$$\mathbf{r}_*^E = \boldsymbol{\mathcal{V}}_k^E \mathbf{f}_{\mathcal{T},*} + \boldsymbol{\mathcal{V}}_k^E \mathbf{L}_k^E \boldsymbol{\Pi}_{k,*}^{\nabla,E} \mathbf{u}_{\mathcal{T}}^E + \boldsymbol{\mathcal{V}}_{k-1}^E \mathbf{D}_{k-1,*}^E \mathbf{p}_{\mathcal{T}}^E \quad \text{for } * \in \{x, y\}.$$

We used the Vandermonde matrix $\boldsymbol{\mathcal{V}}_{k-1}^E$ and the derivative matrix $\mathbf{D}_{k-1,*}^E$ of order $k-1$ for pressure term. These matrices can be simply obtained from those of order k, respectively, by taking the first N_{k-1} columns of $\boldsymbol{\mathcal{V}}_k^E$ and the first N_{k-1} rows and columns of $\mathbf{D}_{k,*}^E$. Then, we compute the jump term over the edges of the element E. For each edge $e \in \mathcal{E}_E$, we denote with the $E' \in \mathcal{T}$ the element such that $\partial E \cap \partial E' = e$. We define the residual jump vectors $\mathbf{j}_x^E, \mathbf{j}_y^E \in \mathbb{R}^{N_q^e}$ as follows

$$\begin{aligned}\mathbf{j}_*^E =& \boldsymbol{\mathcal{V}}_k^E (\mathbf{D}_{k,x}^E \boldsymbol{\Pi}_{k,*}^{\nabla,E} \mathbf{u}_{\mathcal{T}}^E - \mathbf{D}_{k,x}^{E'} \boldsymbol{\Pi}_{k,x}^{\nabla,E'} \mathbf{u}_{\mathcal{T}}^{E'}) n_x^e \\ &+ \boldsymbol{\mathcal{V}}_k^E (\mathbf{D}_{k,y}^E \boldsymbol{\Pi}_{k,*}^{\nabla,E} \mathbf{u}_{\mathcal{T}}^E - \mathbf{D}_{k,y}^{E'} \boldsymbol{\Pi}_{k,x}^{\nabla,E'} \mathbf{u}_{\mathcal{T}}^{E'}) n_y^e - \boldsymbol{\mathcal{V}}_{k-1}^E (\mathbf{p}_{\mathcal{T}}^E - \mathbf{p}_{\mathcal{T}}^{E'}) n_* \quad \text{for } * \in \{x, y\},\end{aligned}$$

where n_x^e and n_y^e denote the components of the normal vector to the edge. The the a posteriori estimator is computed as follows

$$\begin{aligned}\eta(E; \boldsymbol{u}_{\mathcal{T}}, p_{\mathcal{T}})^2 = h_E^2 (\mathbf{w}^E)^T (\mathbf{r}_x^E)^2 + h_E^2 (\mathbf{w}^E)^T (\mathbf{r}_y^E)^2 \\ + \frac{1}{2} \sum_{e \in \mathcal{E}_E} h_E \left[(\mathbf{w}^e)^T (\mathbf{j}_x)^2 + (\mathbf{w}^e)^T (\mathbf{j}_y)^2 \right].\end{aligned}$$

Then, we compute the term $\mathcal{F}(E)$. Since $\boldsymbol{f}$ is a generic L^2 function, this is the only integral we cannot compute exactly. Let $\tilde{\mathbf{f}}_x, \tilde{\mathbf{f}}_y \in \mathbb{R}^{N_q^E}$ be the vector whose components are respectively the x and the y components of the source term evaluated in the quadrature points. The contribution $\mathcal{F}(E)$ is computed as follows

$$\mathcal{F}(E)^2 = (\mathbf{w}^E)^T (\tilde{\mathbf{f}}_x - \mathbf{f}_{\mathcal{T},x})^2 + (\mathbf{w}^E)^T (\tilde{\mathbf{f}}_y - \mathbf{f}_{\mathcal{T},y})^2.$$

Finally, the stabilization term $\eta_{s,E}^2$ is computed by exploiting the linearity of the stabilization operator:

$$S_{\mathcal{T}}^E(\boldsymbol{u}_{\mathcal{T}}, \boldsymbol{u}_{\mathcal{T}}) = (\mathbf{u}_{\mathcal{T}}^E)^T \mathbf{S}_{\mathcal{T}}^E \mathbf{u}_{\mathcal{T}}^E,$$

where $\mathbf{S}_{\mathcal{T}}^E$ is the local stabilization matrix.

Conclusions

In this thesis we have proved that the stabilization term is bounded from the top by the a posteriori error estimator, leading to a stabilization-free upper bound of the total error for the Stokes problem. Moreover, the computation of the a posteriori error estimator has been implemented and tested. Numerical results have shown that the stabilization term can be erased in the a posteriori error estimate, eithout loss of reliability. Thus, the theoretical results obtained are validated. A further development in the AVEM theory for the Stokes problem is to prove that a contraction property holds, ensuring that every iteration of the process implies a reduction of the total error.

Bibliography

[1] Bashir Ahmad, Ahmed Alsaedi, Franco Brezzi, L Donatella Marini, and Alessandro Russo. Equivalent projectors for virtual element methods. *Computers & Mathematics with Applications*, 66(3):376–391, 2013.

[2] L. Beirão da Veiga, C. Canuto, R. H. Nochetto, G. Vacca, and M. Verani. Adaptive vem: Stabilization-free a posteriori error analysis and contraction property. *SIAM Journal on Numerical Analysis*, 61(2):457–494, 2023.

[3] L Beirão da Veiga, F Brezzi, Luisa Donatella Marini, and A Russo. H (div) and h (curl)-conforming vem. *arXiv e-prints*, pages arXiv–1407, 2014.

[4] L Beirão da Veiga, Franco Brezzi, Luisa Donatella Marini, and Alessandro Russo. The hitchhiker's guide to the virtual element method. *Mathematical models and methods in applied sciences*, 24(08):1541–1573, 2014.

[5] Lourenco Beirão da Veiga, Franco Brezzi, Andrea Cangiani, Gianmarco Manzini, L Donatella Marini, and Alessandro Russo. Basic principles of virtual element methods. *Mathematical Models and Methods in Applied Sciences*, 23(01):199–214, 2013.

[6] Stefano Berrone, Andrea Borio, Gioana Teora, and Fabio Vicini. Gedim: Geometry for discretization method library. *Zenodo*, 2025.

[7] Stefano Berrone, Andrea Borio, Gioana Teora, and Fabio Vicini. Polydim: A c++ library for polytopal discretization methods. *arXiv preprint arXiv:2505.14063*, 2025.

[8] Franco Brezzi and Michel Fortin. *Mixed and hybrid finite element methods*, volume 15. Springer Science & Business Media, 2012.

[9] Claudio Canuto and Davide Fassino. Higher-order adaptive virtual element methods with contraction properties. *Mathematics in Engineering*, 5(6), 2023.

[10] L Beirão Da Veiga, Carlo Lovadina, and Giuseppe Vacca. Virtual elements for the navier–stokes problem on polygonal meshes. *SIAM Journal on Numerical Analysis*, 56(3):1210–1242, 2018.

[11] Lourenco Beirão da Veiga, Carlo Lovadina, and Giuseppe Vacca. Divergence free virtual elements for the stokes problem on polygonal meshes. *ESAIM: Mathematical Modelling and Numerical Analysis*, 51(2):509–535, 2017.

[12] Willy Dörfler. A convergent adaptive algorithm for poisson's equation. *SIAM Journal on Numerical Analysis*, 33(3):1106–1124, 1996.

[13] Vivette Girault and Pierre-Arnaud Raviart. *Finite element methods for Navier-Stokes equations: theory and algorithms*, volume 5. Springer Science & Business Media, 2012.

[14] Gaël Guennebaud, Benoit Jacob, et al. Eigen. *URl: http://eigen. tuxfamily. org*, 3(1):8, 2010.

[15] Chris Rycroft. Voro++: A three-dimensional voronoi cell library in c++. 2009.

[16] Giuseppe Vacca. An h 1-conforming virtual element for darcy and brinkman equations. *Mathematical Models and Methods in Applied Sciences*, 28(01):159–194, 2018.

[17] Rüdiger Verfürth. *A posteriori error estimation techniques for finite element methods*. OUP Oxford, 2013.

[18] Gang Wang, Ying Wang, and Yinnian He. A posteriori error estimates for the virtual element method for the stokes problem. *Journal of Scientific Computing*, 84(2):37, 2020.